Bulletin of Entomological Research

Walking behaviour in the ground beetle, Poecilus cupreus: dispersal potential, intermittency and individual variation.

--Manuscript Draft--

Manuscript Number:	BER-D-19-00139R4
Full Title:	Walking behaviour in the ground beetle, Poecilus cupreus: dispersal potential, intermittency and individual variation.
Article Type:	Research Paper
Corresponding Author:	Joseph David Bailey University of Essex Colchester, Essex UNITED KINGDOM
Corresponding Author Secondary Information:	
Corresponding Author's Institution:	University of Essex
Corresponding Author's Secondary Institution:	
First Author:	Joseph David Bailey
First Author Secondary Information:	
Order of Authors:	Joseph David Bailey
	Carly M Benefer
	Rod P Blackshaw
	Edward A. Codling
Order of Authors Secondary Information:	
Abstract:	Dispersal is a key ecological process affecting community dynamics and the maintenance of populations. There is increasing awareness of the need to understand individual dispersal potential to better inform population level dispersal, allowing more accurate models of the spread of invasive and beneficial insects, aiding crop and pest management strategies. Here, fine-scale movements of Poecilus cupreus, an important agricultural carabid predator, were recorded using a locomotion compensator and key movement characteristics were quantified. Net displacement increased more rapidly than predicted by a simple correlated random walk model with near ballistic behaviour observed. Individuals displayed a latent ability to head on a constant bearing for protracted time periods, despite no clear evidence of a population level global orientation bias. Intermittent bouts of movement and non-movement were observed, with both the frequency and duration of bouts of movement varying at the inter- and intra-individual level. Variation in movement behaviour was observed at both the inter- and intra- individual level. Analysis suggests that individuals have the potential to rapidly disperse over a wider area than predicted by simple movement models parametrised at the population level. This highlights the importance of considering the role of individual variation when analysing movement and attempting to predict dispersal distances.

None

Response to Referee Comments: None

Walking behaviour in the ground beetle, *Poecilus cupreus*: dispersal potential, intermittency and individual variation.

Joseph D. Bailey*[1], Carly M. Benefer[2], Rod P. Blackshaw[3], Edward A. Codling[1]

[1]Department of Mathematical Sciences, University of Essex, Colchester, CO4 3SQ, UK.

[2]School of Biological and Marine Sciences, Plymouth University, Plymouth, PL4 8AA.

[3]Blackshaw Research and Consultancy, Parade, Chudleigh, TQ13 0JF.

*Contact author: jbailef@essex.ac.uk

Abstract

Dispersal is a key ecological process affecting community dynamics and the maintenance of populations. There is increasing awareness of the need to understand individual dispersal potential to better inform population level dispersal, allowing more accurate models of the spread of invasive and beneficial insects, aiding crop and pest management strategies. Here, fine-scale movements of *Poecilus cupreus*, an important agricultural carabid predator, were recorded using a locomotion compensator and key movement characteristics were quantified. Net displacement increased more rapidly than predicted by a simple correlated random walk model with near ballistic behaviour observed. Individuals displayed a latent ability to head on a constant bearing for protracted time periods, despite no clear evidence of a population level global orientation bias. Intermittent bouts of movement and non-movement were observed, with both the frequency and duration of bouts of movement varying at the inter- and intra-individual level. Variation in

movement behaviour was observed at both the inter- and intra- individual level. Analysis suggests that individuals have the potential to rapidly disperse over a wider area than predicted by simple movement models parametrised at the population level. This highlights the importance of considering the role of individual variation when analysing movement and attempting to predict dispersal distances.

Keywords: *dispersal, ground beetles, dispersal potential, intermittency, path analysis, random walk.*

1. Background

Dispersal is a key ecological process affecting population, species and community dynamics over small and large spatial scales. For species of ecological and economic importance, such as pest insects and their natural predators, it is essential to understand how dispersal behaviour leads to observed population distributions in order that effective management strategies can be implemented at appropriate scales (Petrovskii et al., 2014).

Ground beetles (Coleoptera: Carabidae) are widely recognised to be important components of terrestrial ecosystems, playing a major role in the food web as both predators of a wide range of invertebrates and as prey to a number of bird and mammal species, some of which are of conservation concern (Holland et al., 2006; Pocock & Jennings, 2007). Carabids are also considered to be of bio-indicative value since they are sensitive to cultivation impacts, and particularly to intensification of agricultural practices (Rainio & Niemelä, 2003). For these reasons, and because of their importance in the natural control of invertebrate pests and weed populations in agricultural land, the biology and ecology of species within

Carabidae have been extensively studied (Bohan et al., 2011; Kromp, 1999). Critical to their function in controlling pest populations within fields is their dispersal ability. Many carabid species are highly mobile with movement mainly via walking, though flight may be used under some circumstances, e.g. longer distance dispersal (Lövei & Sunderland, 1996). Field margins act as refuges for natural enemy species and movement occurs into cropped fields from these semi-natural areas (Thomas et al., 1997). As such, 'beetle banks' have been specifically created in farmland across the UK and Europe as overwintering habitats for beneficial invertebrates (MacLeod et al., 2004; Thomas et al., 1991). Knowledge of dispersal into fields from such areas and the effects of biological characteristics of individual species and how this leads to their observed distribution in agricultural landscapes is key to understanding the maintenance of metapopulations and the dynamics of predator-prey interactions (Banks et al., 2020; Bastola and Davis, 2018; Petrovskii et al., 2014). This is particularly relevant in the context of climate change and habitat fragmentation, for which it is important to be able to predict effects of changes to the environment on species of economic and ecological importance.

Previous studies investigating ground beetle dispersal have used mark-release-recapture techniques (Rijnsdorp, 1980; Thomas et al., 1998, 1997). This approach results in the estimation of movement distance being limited to the maximum distance at which pitfall traps are set. Others have used harmonic radar to track individuals (Lövei et al., 1997; Wallin & Ekbom, 1994). These are similar in principle to mark-release-recapture because individuals are tagged and then located at a later time point. However, neither of these approaches gives fine-scale detail of walking movements since observation frequencies are low and often the majority of individuals released are not recovered. To try to overcome these limitations, individual-based simulation models have been used, incorporating spatial and landscape parameters for forest carabids (Jopp & Reuter, 2005) and common agricultural (*Pterostichus*) species (Benjamin et al., 2008; Firle et al., 1998), or based on population level estimates of random walk movement parameters for a range of insects including ground beetles (Byers, 2001). Although such models may try to take into account factors that are likely to affect distribution and abundance in the field, they are frequently based on data collected from field studies like those described above, which do not explicitly consider inter- and intra-individual variation in walking behaviours and how this affects dispersal distances. This is particularly relevant when considering pest species and their natural predators, since it is important to know the extent of dispersal in differing situations i.e. under alternate cultivation practices. Studies using high resolution movement data in a homogenous featureless environment have been recorded for mealworm beetles (*Tenebrio molitor*) (Reynolds et al., 2013), where a power law distribution in the beetles' step-lengths was found. In the same study, highly linear movements in *Poecilus* beetles were reported, although a full analysis for this species was not undertaken.

Recent advances in tracking technology mean that fine-scale position data can now be more easily collected from real animal movement paths in both the field and laboratory. In this study we used a laboratory based technique, a locomotion compensator, to measure fine-scale walking movements of *Poecilus cupreus*, one of the most common carabid species in European agricultural land (Kromp, 1999; Luff, 2002). It is a diurnal, macropterous species which is active in spring-summer and is found in relatively dry warm habitats such as open grassland and agricultural fields (Luff, 1998). Its abundance and dominance in these habitats makes it an ideal species for investigating movement behaviour within- and between- individuals. Although the locomotion compensator is not a new technique (Kramer, 1976), to our knowledge it has not been used in this way before. It should be noted that the artificial setup of the experiment results in limitations as to the conclusions which can be reliably drawn from these results. Whilst such problems regarding the artificiality and low generality of the setup are a recognised flaw in model systems (Carpenter, 1996) and lead to the common 'replication versus realism' debate (Srivastava et al, 2004; Schindler, 1998) there are inherent benefits of such model systems, such as repeatability and ease of experimentation (Levins, 1984; Srivastava et al, 2004). In this experimental setup the use of the TrackSphere locomotion compensator allows for data to be collected with relative ease and accuracy, giving data with high frequency and greater accuracy than would be expected from simple video analysis or from capture-recapture techniques. Similarly, the setup removes any impedimentary effect a tracker attached to an individual would have.

Here we chose to focus on measuring the dispersal potential of *P. cupreus* as well as discerning whether there were significant differences in general movement patterns in an unobstructed environment. We give a detailed analysis of individual movement of *P. cupreus* which the novel use of the TrackSphere allows. We quantify the observed movement using standard path analysis measures and explore the level of inter- and intra-individual variation. We subsequently demonstrate how simple random walk movement models, parameterised at the population level from the observed data, do not adequately explain the observed dispersal behaviour.

2. Methods

2.1 Insect Collection and Care

Adult *P. cupreus* were captured daily using pitfall traps from a permanent grazed grassland in Dartington, Devon, UK (1.7 acre field, centred at OS grid reference SX 78366 62988) between 8th and 20th July 2012, coinciding with main activity period for this species. Pitfall traps consisted of 200 ml white plastic cups dug into the ground, flush with the soil surface. Each trap was covered by a plastic lid to prevent flooding during wet weather. No preservative or liquid was used inside the pitfall traps in order to retain live individuals. The beetles were maintained at 16^{o}C in tanks containing soil, leaf litter and dead wood in mixed populations with other ground beetle species and fed on fresh meat based (chicken) cat food every few days until needed for the experiment, whereby identified individuals were transferred to separate 20 ml universal tubes containing a small piece of damp tissue paper (Luff, 2002).

2.2 Tracking beetle walking behaviour

2.2.1 Use of TrackSphere

A locomotion compensator (Tracksphere LC 300, Syntech, Hilversum, The Netherlands; Syntech, 2004) was used to track and measure the movement paths (measured in mm) for each beetle. The locomotion compensator consists of a lightweight sphere (300mm diameter), with a camera located directly above to measure displacements. The sphere rotates opposite to these displacements by means of two electric motors, and two encoders contacting the sphere transmit the rotational movements to a computer as incremental (*x*, *y*) coordinates, which are recorded 10 times per second. The sphere is supported by a noiseless aerostatic spherical bearing.

2.2.2 Experimental Design

Beetles were tested three times each between 1st and 8th August 2012. Between trials individuals were maintained at 16°C. Experiments were carried out between 16.8 and 24.2°C, recorded at the beginning of each trial, and were illuminated by a fluorescent light located directly behind the sphere. A white cardboard screen was placed around the sphere to prevent external influences affecting beetle behaviour and the sphere was wiped clean with 70% ethanol after each trial. Individual beetles were allowed to acclimatise on the sphere for one minute before recording began for ten minutes. However, due to the sphere failing to properly compensate for the movements of eight beetles for the full ten minute period, the final analysis was performed on data recorded over a five minute span starting from 10 seconds into the track and finishing 5 minutes later (this period of data collection was available for all experimental trials). Trials in which beetles did not move at all during this period were removed from the dataset completely, giving data from 22 individual beetles. In summary, walking movement data ((x, y) coordinates recorded 10 times per second) over a five minute period were obtained for 22 individual beetles, repeated three times each (66 observations in total).

2.3 Initial processing of movement path data

The raw movement data, recorded at a frequency of 10 Hz was found to include artificial 'pixelisation' of the movement paths, leading to artificially high turning angles being recorded. To overcome this problem, the raw data was sub-sampled at a sampling rate of 1 Hz to smooth the movement paths and avoid pixelisation effects (i.e. only every 10^{th} location recorded in the raw data was included in the analysis). The choice of 1 Hz as the sub-sampling rate was essentially an arbitrary choice, however other sampling rates of 2 Hz, 0.5 Hz and 0.2 Hz (i.e. respectively only every 5^{th}, 20^{th} or 50^{th} raw data point included) were also considered but did not qualitatively change the results (Supplementary Tables S1-10, Additional File 3).

A minimum instantaneous speed threshold was used to classify bouts of 'purposeful movement' (movement associated with relocation in space) and 'non-movement' (periods where beetles either paused to reorient or stopped moving entirely, leading to zero or limited relocation in space). This gave an objective way to classify each step of the movement paths with instantaneous speeds above the minimum threshold classified as movement and those below as periods of non-movement. A range of minimum speed threshold values were considered: 5 mm/s, 10 mm/s and 15 mm/s, as well as no minimum speed threshold. The minimum speed threshold of 5 mm/s was used for the main analysis as this retained the largest number of data points while allowing objective classification of bouts. The use of different minimum speed thresholds did not lead to qualitatively different results (Supplementary Tables S1-10, Additional File 3).

Using this threshold (5 mm/s) lead to movement and stationary bouts of very short length due to noise in the recording and processing of the data. To account for this the movement data were smoothed, with bouts of movement and non-movement identified using a cumulative sum algorithm similar to Knell & Codling (2012) (see Additional File 1). Bouts that had not ended by the end of the experiment were considered to have been artificially truncated and hence were not included in the analysis presented in the main paper, since their true duration was indeterminable. However, results were qualitatively similar if these truncated bouts were included, under the assumption that they terminated at the end point of the experiment (see Additional File 4).

%%Figure 1 about here%%

2.4 Statistical analysis

2.4.1 Basic Path analysis measures

Standard path analysis measures adopted from random walk theory were quantified for each of the observed movement paths (Kareiva & Shigesada, 1983; Kramer & McLaughlin, 2001; Goodwin & Fahrig, 2002; Codling et al, 2008). It is known that the precise form of the distributions underlying movement in step-turn processes has large effects on the predicted movement and hence a detailed analysis of individual movement is required in order to accurately predict movement behaviour (Codling et al, 2010; Choules & Petrovskii, 2017). Therefore, for each movement path the turning angles between the directions of successive movement steps, the global direction of movement at each step, and step length / speed (step length and the instantaneous speed are equivalent as we used a fixed sampling frequency of 1 Hz), were calculated (Figure 1C-D). The observed speeds were then used to determine bouts of movement and non-movement as described in the previous section. Summary statistics for each movement path were determined: total net displacement (mm; Figure 1B), mean cosine of turning angles, straightness (total track length/total net displacement; a measure of tortuosity), average speed (mm/s; determined for bouts of movement only), number of bout transitions (movement to non-movement and vice versa), average bout duration (s), variance in bout duration (s^2), and proportion of time spent moving (%). Temperature was included as a covariate in the initial analyses but was found not to be significant and so was excluded from subsequent analysis, as has been observed in other studies of ground beetle movement (Tuf et al. 2012; Růžičková & Veselý, 2016).

2.4.2 Intra- and inter-individual variation

Repeatability

To measure the consistency of behaviour among individuals the repeatability, r, was calculated (also known as the intra class coefficient, ICC, (Lessels & Boag, 1987)). Where $r = V_{\mathrm{ind}}/(V_{\mathrm{ind}} + V_{\varepsilon})$ with V_{ind} being the variance between individuals and V_{ε} the residual variance, which is equivalent to the variation within individuals (Nakagawa & Schielzeth, 2010; Dingemanse & Dochtermann, 2013; Houslay & Wilson 2017). Therefore, r, indicates the relative strength of the variance between individuals compared to the total variance ($V_{\mathrm{ind}} + V_{\varepsilon}$) (Brommer, 2013; Dingemanse & Dochtermann, 2013; Dosmann et al. 2015). These variances were found using Linear Mixed Effect Models using Restricted Maximum-Likelihood parameter estimation following the method described in Nakagawa & Schielzeth (2010) by use of the *rptR* package (Stoffel et al, 2017) in *R* (R Core Team, 2018).

Correlation

Correlation between any of the parameters at either the between- or within-individual level was calculated by dividing the covariance between two parameters by the square root of the product of the two variances (Dosmann et al, 2015). These values we found using a bivariate (two-trait) mixed model, with the individual beetle as the random intercept, the experiment number (centred) as the repeat number, and the parameters (centred and scaled) as the random effects, as per Houslay & Wilson (2017). The model was implemented by the MCMCglmm package (Hadfield, 2010) in R (R Core Team, 2018). In order to ensure auto-correlation was not an effect, 500,000 iterations were run with a 'burn-in' period of 15,000 and a thinning of 100. Results were significant if the confidence intervals (95%) did not span 0, as is standard with Bayesian CI's (Houslay & Wilson 2017).

2.4.3 Global Movement Direction

Global orientation of movement directions were considered at both population and individual level, to ascertain whether a global or an individual preference in direction existed. A Watson test checked for uniform distribution of global movement directions and a Rayleigh test determined whether the distribution corresponded to a unimodal wrapped distribution with specific resultant vector (where a resultant vector close to 1 would indicate a strong preference in movement direction, whereas a vector close to 0 would indicate no preference in direction).

2.4.4 Turning Angles

The observed turning angles were fitted to two standard circular probability distributions: the von Mises (a close approximation to the normal distribution on a circle) and the wrapped Cauchy (a heavy-tailed circular distribution). These were fitted using the CircStats package in *R* (R Core Team, 2018). The Kuiper and the Watson-U^2 tests were used to check the validity of both models, with the Akaike Information Criterion (AIC) used to indicate the closer fitting distribution (Mardia & Jupp, 2009). Evidence of unimodal turning angle distributions centred around 0 would indicate persistence in the beetles' movements.

2.4.5 Step lengths (instantaneous speeds) & Intermittency

Four distributions were considered for fitting the observed distribution of step lengths (instantaneous speeds), with the same distributions also considered for the movement and non-movement bout durations: power-law, exponential, Weibull and log-normal. Distributions were fitted using the *fitdistrplus* package in *R* (R Core Team, 2018), except for the power-law that was fitted using the *power.law.fit* function in the iGraph package in *R* (R Core Team, 2018). The power-law was considered in two circumstances. Firstly, to check if a power-law fitted all the data, a restricted power-law was considered. The x_{min} value in this case was set at the smallest non-zero value of the data rather than the value for x_{min} calculated by *power.law.fit* function (Virkar & Clauset, 2014). Secondly, a power-law fitting only the tail of the data was considered as this is an indicative features of Lévy walk behaviour (Edwards et al., 2007; Sims et al., 2007; Reynolds et al., 2013; Ahmed et al., 2018). The tail of the data was calculated by using the best fit x_{min} value calculated by the *power.law.fit()* function. The potential distributions were fitted only to data points which were greater than this minimum value. As the fitting algorithm for the power-law utilised a maximum likelihood estimation (MLE) method to maximise the p-value for the Kolmogorov–Smirnov (K-S) test, a G-test was also used to consider the fit of the distributions (Edwards et al., 2007).

2.4.6 CRW v BRW Behaviour

To investigate whether the characteristics of the beetle movement paths could be classified best as either a correlated random walk (CRW; i.e. movement is persistent but not globally directed) or a biased random walk (BRW; i.e. movement is globally directed), we measured the Δ statistic from (Marsh & Jones, 1988):

$$\Delta = \frac{1}{n^2}\left[\left(\sum \cos\theta_i\right)^2 + \left(\sum \sin\theta_i\right)^2\right] - \frac{1}{(n-1)^2}\left[\left(\sum \cos\omega_i\right)^2 + \left(\sum \sin\omega_i\right)^2\right] \quad (1)$$

where, θ_i is the global orientation and ω_i is the turning angle, at time i. The Δ statistic gives a relative measure of how well the observed data fits each of the two types of random walk movement model (see details in Additional File 5).

Data for turning angles and step lengths (speeds) were fitted at the population level (10045 data points from 66 movement paths) and at the individual path level (between 37 and 298 data points for each movement path). The Δ statistic was calculated for each individual movement path separately and also for all turning and global orientation angles aggregated at the population level. Data for bout durations were fitted only at the population level due to the limited number of data points from each individual path (326 data points from 66 movement paths).

3. Results

3.1 Basic path analysis measures

Figure 1C illustrates how the observed movement paths consisted of bouts of high speed and highly persistent movement (where the mean cosine of turning angles is close to 1), interspersed with bouts of low speed (5-10 mm/s) in which the distribution of turning angles is more uniform.

The beetles' net displacement ranged from 14 to 9785 mm (Figure 2A) with the measure of straightness of each individual path varying from 0.98 (near straight-line movement) to 0.21 (tortuous) (Additional File 2; Supplementary Figure S1). The average of the mean cosine values was found to be 0.780 with a standard deviation of 0.146, indicating a small range of values for the mean cosine across all trials (Figure 2C). On average the beetles as a population spent 55.5% of the experiment moving, recording an average speed when moving in the range of 5.65 mm/s to 36.3 mm/s with the population average being 12.5 mm/s (Figure 2B; Additional File 2, Supplementary Figure S1). The number of transitions from bouts of movement to non-movement (and vice-versa) in a single trial varied from 0 to 12 across the population, with individuals exhibiting a wide range in the number of transitions across their individual 3 trials (Figure 2D). Correspondingly the average bout length varied from 17s, for the individual trial which displayed 12 completed bouts, to 293s for the individual trial which displayed only one complete bout during the experiment.

3.2 Intra- and inter-individual variation

Repeatability

The number of bouts, time spent moving (%) and average speed when moving were found to be repeatable implying that the beetles displayed individual consistency across the three trials. ($p < 0.05$). All of these gave a repeatability of over 0.2, with the highest being average speed when moving, $r = 0.282$. However, when considering the 95% confidence intervals, only average speed had an interval which did not span 0, indicating that average speed was the only consistent movement behaviour (Table 1).

The repeatability results demonstrate that between 12.7-36.2% of the variance in the parameters was caused by differences between individuals and therefore the majority of the variation in the parameters is due to the differences within-individuals (Additional File 2; Table S1).

% Table 1 about here %

Correlation in parameters

At the between individual level all parameter combinations had CI's which span 0 indicating no evidence of statistically significant correlation (Additional File 2; Table S2). At the within-individual level, a strong positive correlation ($p < 0.01$) between displacement, straightness and time spent moving was observed, as well as between displacement and average speed, as might be expected from standard movement. A strong negative correlation ($p < 0.01$) between the average bout duration and the number of bout transitions was anticipated: the longer a bout, the fewer there can be in a given time period. However, a significant positive correlation ($p < 0.01$) between the average speed when moving and the time spent moving was also found, indicating that the longer the time the beetles spent moving, the faster on average they moved (Additional File 2; Table S3).

% Figure 2 about here %

3.3 Global movement direction

Figure 1D shows a near uniform distribution in the global orientation angle, relative to the associated turning angle for the pooled data across all beetles and trials. This suggests that, at the population level, there is no consistent reorientation towards a specific global movement direction. A Rayleigh test at the population level revealed a slight bias towards a global movement direction of $\bar{\mu} = 59°$, although the resultant vector was low ($\bar{R} = 0.194$) suggesting this was only a weak effect

At the individual level, beetles were observed to have highly consistent oriented movements (resultant vector, $\bar{R}$, ranging from 0.194 to 0.972, with $\text{mean} = 0.662, \text{sd} = 0.213$). The Watson test rejected the possibility of a uniform distribution of global movement directions for each individual, indicating movement at the individual level was highly directed.

3.4 Turning Angles

When considering the distribution of turning angles at the population level, both the wrapped Cauchy (MLE parameters: ρ=0.859, μ=0.005) and von Mises distributions (MLE parameters: $\kappa = 6.43, \mu = 0.001$) were rejected by the Watson test ($U^2_{wc} = 2.42, p < 0.01$; $U^2_{vM} = 51.9, p < 0.01$) and the Kuiper test ($V_{wc} = 6.79, p < 0.01$; $V_{vM} = 21.1, p < 0.01$) (Supplementary Tables S1-S2, Additional File 3). However, the AIC favoured the wrapped Cauchy over the von Mises ($AIC_{wc} = 7032, AIC_{vM} = 10668$), and visual inspection indicates that the wrapped Cauchy is the better fit (Figure 3A). Tests at other sampling rates and speed thresholds revealed no significant differences from these results (Supplementary Tables S1-S2, Additional File 3).

At the individual level, a wrapped Cauchy distribution was found to be the best fitting distribution for 58 of the 66 trials. The resultant vectors for each of the individual trials were high, indicating persistence in movement ($\bar{R}$ ranging from 0.397 to 0.913 with $\text{mean} = 0.780,\ \text{sd} = 0.147$).

3.5 Step-lengths (Instantaneous speeds) & Intermittency

When considering the distribution of the instantaneous speeds at the population level, both the Kolmogorov-Smirnov (K-S) test and G-test rejected all four distributions ($p < 0.01$) when fitted to the tail of the data. The AIC indicated that the Weibull distribution (MLE parameters; $\gamma = 0.992, \alpha = 9.67$) was the closest fit (Supplementary Tables S3-S5, Additional File 3). When considering the full data set and using a restricted power-law with $x_{min} = 5$, the K-S test and G-test still rejected all the distributions ($p < 0.01$), but the AIC now favoured the log-normal distribution (Figure 3B) with MLE parameters $\mu = 1.69, \sigma^2 = 1.28$ (Supplementary Tables S6-S8, Additional File 3). Choosing different values for the sampling rate and speed threshold did not qualitatively change these results (Supplementary Tables S3-S8, Additional File 3). At the individual level, the log-normal and the Weibull distributions were favoured in 65 of the 66 trials when considering the full data set, and 61 of the 66 when looking only at the tail of the data.

3.6 Intermittency (movement and non-movement bouts)

Both the Weibull (MLE parameters; $\gamma = 0.97, \alpha = 45.7$) and log-normal (MLE parameters; $\mu = 3.30, \sigma^2 = 1.04$) distributions were accepted by the G-test for the distribution of the bouts of movement with the AIC value distinguishing between them by favouring the log-normal distribution. For the bouts of non-movement, the G-test and K-S test reject all the distributions ($p < 0.01$); although, the log-normal distribution (MLE parameters; $\mu = 3.00, \sigma^2 = 0.94$) was favoured by the AIC ($\text{AIC}_{\text{log-norm}} = 1373$, $\text{AIC}_{\text{exp}} = 1420$, $\text{AIC}_{\text{weib}} = 1422$). Visual inspection implies a reasonable fit here (Figures 3C-D; Supplementary Tables S9-S10, Additional File 3).

As predicted by the lognormal distribution an inverse relation was found between lengths of following bouts, with a long bout often followed by a short bout, and bouts close to the median bout length mostly followed by bouts of comparable length (Additional File 3, Supplementary Figure S1).

% Figure 3 about here %

3.7 CRW v BRW behaviour

At the individual level the Marsh-Jones Δ statistic indicated that the observed data did not fit with the expected result from either a CRW or BRW, with 60 paths giving an indeterminate result, 5 paths identified as most like a CRW and only one most like a BRW (Additional File 5; Supplementary Table S1). Similarly, at the population level, the statistic did not coincide with the expected result for either a BRW or a CRW. However, in this case the value ($\Delta = -0.335$) was strongly negative and much closer to the expected CRW value, indicating that the population movement was more similar to a CRW.

When the observed net displacement was compared with the expected displacement of a CRW (parameterised by calculated population level values of the speed and turning angle mean resultant length), it is clear that the beetles dispersed considerably faster than expected by simple CRW movement (Figure 4). With an initial period of super-ballistic behaviour followed by a sustained linear increase in net displacement over time as predicted by a purely ballistic movement process.

% Figure 4 about here %

4 Discussion

Movement data of 22 *P. cupreus* beetles were collected over three replicate trials on a locomotion compensator. Analysis of observed trajectories highlighted high levels of inter- and intra-individual variation in movement path characteristics (Figure 1 & 2), with a correlation between time spent moving and instantaneous speed, suggestive of possible ‘flee’ behaviour. Observed turning angles were best fitted by the wrapped Cauchy distribution with step lengths (instantaneous speeds) best described by a log-normal distribution with no evidence of power-law behaviour (Figure 3A-B). Beetle movements were observed to be highly persistent at the individual level, with beetles able to maintain forward movement towards a chosen direction over a sustained period. At the population level, a weak preference in global movement direction appeared to be present, however, further inspection highlighted that this weak global directional bias was directly correlated to the initial movement direction of the beetles at the start of recording, (presumably related to the initial orientation of the beetle as they were released onto the tracking sphere’), and the global bias towards this specific orientation had disappeared by the end of each trial (Additional File 5; Supplementary Figure S1). Hence, there was no strong evidence for a consistent global bias at the population level (see Figure 1A). This could be an artefact of the experimental setup where such an unfamiliar setting caused the beetles to engage in ’flee’ behaviour where movement was in a constant direction away from the starting location. Assuming the beetles were not placed facing exactly the same direction at the start of the experiment, along with the beetles' inherent ability to travel in a straight line could explain the lack of global direction.

Intermittency in movement was observed, with the lengths of the bouts of movement and non-movement both best described by log-normal distributions (Figure 2C-D). Movement bouts were found to highly vary between individuals at both the inter- and intra-individual level, with some trials consisting of bouts of constant movement and others involving highly intermittent stop-start behaviour. The intermittency in movement behaviour, along with the observation that bouts of short length are often followed by bouts of similar length (Additional File 3, Figure S1), has been characterised as foraging or searching behaviour in aphids (Mashanova et al, 2010) and has been reported for a number of species including crickets, copepods and ghost crabs (Kramer & McLaughlin, 2001).

The ability for individual beetles to disperse over much larger distances than predicted by a simple CRW movement model, while showing no evidence of a global preferred direction at the population level, is an interesting finding. The beetles in this study showed an innate ability to travel on a near constant bearing with high persistence (Figure 1A) a phenomena found in other insects such as dung beetles (Byrne et al, 2003) but has been shown to not be present in other animals such as humans (Souman et al, 2009). It is known that small errors in attempted straight line movement compound over time (Biegler, 2000; Cheung et al, 2007), therefore, if an individual can continue on a constant bearing for a protracted time period without any obvious external cues, the method by which these small errors are negated is interesting and may be due to some unknown internal cue. Similar underestimates of total displacement have also been reported when considering parameterised CRW models for *T. confusum* beetles (Morales & Ellner, 2002) and three *Eleodes sp.* (Crist et al, 1992). A possible explanation for these discrepancies is that the parameterised models do not consider the use of internal mechanisms or external cues that enable deviations in heading to be corrected so that forward movement is maintained. However, it is far from clear in this context what such mechanisms might be since there were no known visual navigation cues in the immediate walled environment of the locomotion compensator that could have been utilised.

Other insect species, such as bumblebees and other arthropods, (Chittka et al, 1999; and references therein) are thought to possess an internal magnetic compass that allows forward navigation in the absence of other cues. Bumblebees also use odour cues to direct movement within a featureless environment (Chittka et al, 1999) and are able to discriminate between hydrocarbon scent marks excreted from the tarsi left by themselves and conspecifics on flowers (Pearce et al, 2017); *P. cupreus* has been observed to use chemical cues to navigate, orienting towards prey such as *Heteromurus nitidus*, a ground dwelling springtail (Mundy et al, 2000) therefore a similar mechanism might allow them to track their own footprints on the locomotion compensator, although we have no direct evidence that this is the case.

Polarization of light has been shown to act as a method of navigation in many species of insect and beetles (Scwhind, 1991; Wehner, 2001). Dung beetles (e.g. *Scarabaeus sp.* and *Scarabaeini sp*) have been shown to use the polarisation of light to move with high persistence (Dacke et al, 2004; Baird et al, 2012), Although there were no direct visual cues in our experimental arena, there was a fixed light source on the ceiling of the laboratory and it is possible that *P. cupreus* are using the polarisation of the light source relative to their initial starting direction to maintain their forward movement. This could be simply tested by running a similar experimental setup incorporating a light polariser, similar to the method used to demonstrate the use of light polarisation in dung beetle navigation (Dacke et al, 2004; Baird et al, 2012).

Whilst the experimental setup allowed for the collection of data both at a high frequency and high level of accuracy, giving answers to the questions regarding the dispersal potential and variability in movement behaviour of *P. cupreus*, the experimental setup itself causes the conclusions and applications of our findings to be limited. Due to the featureless conditions, caution must be taken in generalising these results as they are not indicative of movement in natural environments, in which encounters with obstacles or changing conditions would be present. However, a similar tracking device was used in Dahmen et al, 2018 to compare the movement of desert ants (*Cataglyphis sp.*) under experimental conditions to those observed in an open test field. They recorded movement in a test arena both outside with natural light and inside a laboratory with a polarised light source, comparing the observed movement to that recorded by using a cushioned tracking sphere under similar conditions. The findings reported no significant differences between the movement recorded using the tracking sphere to that in the open test field. Whilst this may be the case for this specific species of ant, as we did not engage in similar direct comparisons of movement in natural settings to that on the TrackSphere, it is not necessarily clear that movement recorded on such a device can act as a sensible approximation for real world movement

Although the homogeneity of the experimental setup has been highlighted as a flaw in scaling up our findings to movement in the real world, the agricultural landscapes *P. cupreus* often inhabit, are by their cultivated nature more homogeneous relative to non-agricultural landscapes. Therefore, our recorded movement behaviour could be beneficial to studies which attempt to understand the invasive potential of *P. cupreus* in crop management.

Banks et al (2020) looked at the expected affect ladybirds and *P. cupreus* had on controlling aphid invasions of agricultural fields, with the aim of providing a pest management structure to efficiently eradicate aphid populations. Their model concluded that using a population of ladybirds was the most effective compared to a mixture of the two predators. However, the model explicitly relied on predicted movement rates of *P. cupreus* which had been aggregated at the population level. Therefore, applying our findings of the dispersal potential and movement behaviour in similar studies may affect the outcome, leading to alternative crop management strategies.

References:

Ahmed DA, Petrovskii SV and Tilles PFC (2018) The "Lévy or Diffusion" controversy: how important is the movement pattern in the context of trapping? *Mathematics* **6**, 77.

Baird E, Byrne MJ, Smolka J, Warrant EJ and Dacke M (2012). The dung beetle dance: an orientation behaviour? *PLoS One* **7**, e30211.

Banks JE, Laubmeier AN and Banks HT (2020) Modelling the effects of field spatial scale and natural enemy colonization behaviour on pest suppression in diversified agroecosystems. *Agricultural and Forest Entomology* **22**, 30-40.

Bastola A and Davis JA (2018) Determining in-field dispersal of the redbanded stink bug (Hemiptera: Pentatomidae) in soybean fields using a protein based mark-capture method. *Crop Protection* **112**, 24–32.

Benjamin R, Cédric G and Pablo I (2008) Modeling spatially explicit population dynamics of *Pterostichus melanarius* (Coleoptera: Carabidae) in response to changes in the composition and configuration of agricultural landscapes. *Landscape and Urban Planning* **84**, 191–199.

Biegler R (2000) Possible uses of path integration in animal navigation. *Animal Learning & Behavior* **28**, 257-277.

Bohan DA, Boursault A, Brooks DR and Petit S (2011) National-scale regulation of the weed seedbank by carabid predators. *Journal of Applied Ecology* **48**, 888–898

Brommer JE (2013) On between-individual and residual (co) variances in the study of animal personality: are you willing to take the "individual gambit"? *Behavioral Ecology and Sociobiology* **67**, 1027-1032

Byrne M, Dacke M, Nordström P, Scholtz C and Warrant E (2003) Visual cues used by ball-rolling dung beetles for orientation. *Journal of Comparative Physiology A* **189**, 411-418.

Byers JA (2001) Correlated random walk equations of animal dispersal resolved by simulation. *Ecology* **82**, 1680–1690.

Carpenter SR (1996) Microcosm experiments have limited relevance for community and ecosystem ecology. *Ecology* **77**, 677-680

Cheung A, Zhang S, Stricker C and Srinivasan MV (2007) Animal navigation: the difficulty of moving in a straight line. *Biological Cybernetics* **97**, 47-61.

Chittka L, Williams NM, Rasmussen H and Thomson JD (1999) Navigation without vision: bumblebee orientation in complete darkness. *Proceedings of the Royal Society of London. Series B: Biological Sciences* **266**, 45-50.

Choules JD and Petrovskii S (2017) Which random walk is faster? Methods to compare different step length distributions in individual animal movement. *Mathematical Modelling of Natural Phenomena* **12**, 22-45.

Codling EA, Plank MJ and Benhamou S (2008) Random walk models in biology. *Journal of the Royal Society Interface* **5**, 813-834.

Codling EA, Bearon RN and Thorn GJ (2010) Diffusion about the mean drift location in a biased random walk. *Ecology* **91**, 3106-3113

Crist TO, Guertin DS, Wiens JA and Milne BT (1992) Animal movement in heterogeneous landscapes: an experiment with *Eleodes* beetles in shortgrass prairie. *Functional Ecology*, 536-544.

Dacke M, Byrne MJ, Scholtz CH and Warrant EJ (2004) Lunar orientation in a beetle. *Proceedings of the Royal Society of London. Series B: Biological Sciences* **271**, 361-365.

Dahmen H, Wahl VL, Pfeffer SE, Mallot HA and Wittlinger M (2017) Naturalistic path integration of *Cataglyphis* desert ants on an air-cushioned lightweight spherical treadmill. *Journal of Experimental Biology* **220**, 634-644.

Dingemanse NJ and Dochtermann NA (2013) Quantifying individual variation in behaviour: mixed-effect modelling approaches. *Journal of Animal Ecology* **82**, 39-54

Dosmann AJ, Brooks KC and Mateo JM (2015) Within-individual correlations reveal link between a behavioral syndrome, condition, and cortisol in free-ranging belding's ground squirrels. *Ethology* **121**, 125-134.

Edwards AM, Phillips RA, Watkins NW, Freeman MP, Murphy EJ, Afanasyev V, Buldyrev SV, Luz MGE, Raposo EP, Stanley HE and Viswanathan GM (2007) Revisiting Lévy flight search patterns of wandering albatrosses, bumblebees and deer. *Nature* **449**, 1044–1048.

Firle S, Bommarco R, Ekbom B and Natiello M (1998) The influence of movement and resting behavior on the range of three carabid beetles. *Ecology* **79**, 2113–2122.

Goodwin BJ and Fahrig L (2002) Effect of landscape structure on the movement behaviour of a specialized goldenrod beetle, *Trirhabda borealis*. *Canadian Journal of Zoology* **80**, 24-35

Hadfield JD (2010) MCMC methods for multi-response generalized linear mixed models: the MCMCglmm R package. *Journal of Statistical Software* **33**, 1-22.

Holland JM, Hutchison MAS, Smith B and Aebischer NJ (2006) A review of invertebrates and seed-bearing plants as food for farmland birds in Europe. *Annals of Applied Biology* **148**, 49–71.

Houslay TM and Wilson AJ (2017) Avoiding the misuse of BLUP in behavioural ecology. *Behavioral Ecology* **28**, 948-952.

Jopp F and Reuter H (2005) Dispersal of carabid beetles—emergence of distribution patterns. *Ecological Modelling*, Emergent Properties in Individual-based Models Case Studies from the Bornhöved Project (Northern Germany) **186**, 389–405.

Kareiva PM and Shigesada N (1983) Analyzing insect movement as a correlated random walk. *Oecologia* **56**, 234-238.

Knell AS and Codling EA (2012) Classifying area-restricted search (ARS) using a partial sum approach. *Theoretical Ecology* **5**, 325–339.

Kramer E (1976) The orientation of walking honeybees in odour fields with small concentration gradients. *Physiological Entomology* **1**, 27–37.

Kramer DL and McLaughlin RL (2001) The behavioral ecology of intermittent locomotion. *American Zoologist* **41**, 137-153.

Kromp B (1999) Carabid beetles in sustainable agriculture: a review on pest control efficacy, cultivation impacts and enhancement. *Agriculture, Ecosystems & Environment* **74**, 187–228.

Lessells CM and Boag PT (1987) Unrepeatable repeatabilities: a common mistake. *The Auk* **104**, 116-121.

Levins R (1966) The strategy of model building in population biology. *American scientist* **54**, 421-431.

Lövei GL and Sunderland KD (1996) Ecology and behavior of ground beetles (Coleoptera: Carabidae). *Annual Review of Entomology* **41**, 231–256.

Lövei GL, Stringer IAN, Devine CD and Cartellieri M (1997) Harmonic radar - A method using inexpensive tags to study invertebrate movement on land. *New Zealand Journal of Ecology* **21**, 187–193.

Luff ML (2002) Carabid assemblage organization and species composition, in: Holland JM (ed.), *The Agroecology of Carabid Beetles*. Intercept, Andover, UK, pp. 41–80.

Luff ML (1998) *Provisional atlas of the ground beetles (Coleoptera: Carabidae) of Britain*. Biological Records Centre, Institute of Terrestrial Ecology, Monks Wood, Abbots Rip-ton, UK

MacLeod A, Wratten SD, Sotherton NW and Thomas MB (2004) 'Beetle banks' as refuges for beneficial arthropods in farmland: long-term changes in predator communities and habitat. *Agricultural and Forest Entomology* **6**, 147–154.
Mardia KV and Jupp PE (2009) Directional statistics (Vol. 494). John Wiley & Sons.
Marsh LM and Jones RE (1988) The form and consequences of random walk movement models. *Journal of Theoretical Biology* **133**, 113–131.
Mashanova A, Oliver TH and Jansen VA (2009) Evidence for intermittency and a truncated power law from highly resolved aphid movement data. *Journal of the Royal Society Interface* **7**, 199-208
Morales JM and Ellner SP (2002) Scaling up animal movements in heterogeneous landscapes: the importance of behavior. *Ecology* **83**, 2240-2247
Mundy CA, Allen-Williams LJ, Underwood N and Warrington S (2000) Prey selection and foraging behaviour by *Pterostichus cupreus L.* (Coleoptera: Carabidae) under laboratory conditions. *Journal of Applied Entomology* **124**, 349-358..
Nakagawa S and Schielzeth H (2010) Repeatability for Gaussian and non-Gaussian data: a practical guide for biologists. *Biological Reviews* **85**, 935-956.
Pearce RF, Giuggioli L and Rands SA (2017) Bumblebees can discriminate between scent-marks deposited by conspecifics. *Scientific reports* **7**, 43872.
Petrovskii S, Petrovskaya N and Bearup D (2014) Multiscale approach to pest insect monitoring: Random walks, pattern formation, synchronization, and networks. *Physics of Life Reviews* **11**, 467–525.
Pocock MJO and Jennings N (2007) Testing biotic indicator taxa: the sensitivity of insectivorous mammals and their prey to the intensification of lowland agriculture. *Journal of Applied Ecology* **45**, 151–160.
R Core Team (2018) R: A language and environment for statistical computing. R Foundation for Statistical Computing, Vienna, Austria. URL http://www.R-project.org/
Rainio J and Niemelä J (2003) Ground beetles (Coleoptera: Carabidae) as bioindicators. *Biodiversity and Conservation* **12**, 487–506.
Reynolds AM, Leprêtre L and Bohan DA (2013) Movement patterns of *Tenebrio* beetles demonstrate empirically that correlated-random-walks have similitude with a Lévy walk. *Scientific Reports* **3**, 3158.
Rijnsdorp AD (1980) Pattern of movement in and dispersal from a *dutch* forest of *Carabus problematicus* Hbst. (Coleoptera, Carabidae). *Oecologia* **45**, 274–281
Růžičková J and Veselý M (2016) Using radio telemetry to track ground beetles: movement of *Carabus ullrichii*. *Biologia* **71**, 924-930.
Schindler DW (1998) Whole-ecosystem experiments: replication versus realism: the need for ecosystem-scale experiments. *Ecosystems* **1**, 323-334.
Schwind R (1991) Polarization vision in water insects and insects living on a moist substrate. *Journal of Comparative Physiology A* **169**, 531-540.
Sims DW, Righton D and Pitchford JW (2007) Minimizing errors in identifying Lévy flight behaviour of organisms. *Journal of Animal Ecology* **76**, 222–229.
Souman JL, Frissen I, Sreenivasa MN and Ernst MO (2009) Walking straight into circles. *Current Biology* **19**, 1538-1542.
Srivastava DS, Kolasa J, Bengtsson J, Gonzalez A, Lawler SP, Miller TE, Munguia P, Romanuk T, Schneider DC and Trzcinski MK (2004) Are natural microcosms useful model systems for ecology? *Trends in Ecology & Evolution* **19**, 379-384
Stoffel MA, Nakagawa S and Schielzeth H (2017) rptR: Repeatability estimation and variance decomposition by generalized linear mixed-effects models. *Methods in Ecology and Evolution* **8**, 1639-1644.

Syntech (2004) TrackSphere Locomotion Compensator model LC-300. User guide. Syntech Hilversum, The Netherlands.

Thomas CFG, Green F and Marshall EJP (1997) Distribution, dispersal and population size of the ground beetles, *Pterostichus melanarius* (Illiger) and *Harpalus rufipes* (Degeer) (Coleoptera, Carabidae), in field margin habitats. *Biological Agriculture & Horticulture* **15**, 337–352.

Thomas CFG, Parkinson L and Marshall EJP (1998) Isolating the components of activity-density for the carabid beetle *Pterostichus melanarius* in farmland. *Oecologia* **116**, 103–112.

Thomas MB, Wratten SD and Sotherton NW (1991) Creation of "island" habitats in farmland to manipulate populations of beneficial arthropods: predator densities and emigration. *Journal of Applied Ecology* **28**, 906–917

Tuf IH, Dedek P and Veselý M (2012) Does the diurnal activity pattern of carabid beetles depend on season, ground temperature and habitat? *Archives of Biological Sciences* **64**, 721-732.

Wehner R (2001) Polarization vision–a uniform sensory capacity? *Journal of Experimental Biology* **204**, 2589-2596.

Virkar Y and Clauset A (2014) Power-law distributions in binned empirical data. *The Annals of Applied Statistics* **8**, 89–119.

Wallin H and Ekbom B (1994) Influence of hunger level and prey densities on movement patterns in three species of *Pterostichus* beetles (Coleoptera: Carabidae). *Environmental Entomology* **23**, 1171–1181.

Figures

Figure 1 (A) Individual beetle movement paths for the first trial run of each beetle. Starting points are the origin (0,0). **(B)** Displacement over time for each individual beetle from their first trial run. **(C)** Cosine of the turning angle (the angle between successive steps) against the instantaneous speed at that step. The vertical lines represent possible values for the speed threshold value (5 mm/s, 10 mm/s and 15 mm/s) which were used to distinguish between purposeful movement and non-movement. Data is taken for all beetles across all three trials. **(D)** Global orientation of movement at each step (and the cosine of the corresponding turning angle (the angle between successive global orientations). Data is taken for all beetles across all three trials. In all plots the same hue is used to indicate individual beetles. For all figures the sampling size used was 1 Hz.

Figure 2 (A-D) (A) Total displacement, (B) mean cosine of turning angle, (C) mean speed when moving, and (D) number of bout transitions of each beetle for each trial (figures displaying variability across the other parameters are found in Additional File 2, Figure S1). In all plots, circle points correspond to Trial 1, square to Trial 2 and triangle to Trial 3.

Figure 3 (A) Histogram of the turning angles. The solid dark grey line shows the best fit wrapped Cauchy (WC) distribution with $\mu = 0.005, \rho = 0.859$ and the dashed light grey line shows the best fit von Mises (vM) distribution with $\mu = 0.001$ and $\kappa = 6.43$. **(B)** Histogram for distribution of the instantaneous speeds. The grey dashed line shows the best fitting log-normal distribution **(C)** & **(D)** Histograms showing the distribution of the length of bouts of movement and non-movement. The grey dashed line shows the best fitting log-normal distribution. In all cases, the sampling rate was 1 Hz and speed cut-off threshold was 5 mm/s

Figure 4 Net displacement of beetles over time. The solid black line shows the mean net displacement of the beetle population with sampling rate 1 Hz and no speed threshold; the light grey dashed line is the expected result for a CRW with turning angles taken from a zero centred wrapped Cauchy distribution with concentration parameter $\rho = 0.819$, and step length drawn from the exponential distribution with mean, $1/\lambda = 8.33$ (Additional File 3, Supplementary Table S2 & S5); the dark grey dotted line is ballistic movement.

Tables

	Repeatability		
	r-stat	CI (95%)	p-value
Number of Bouts	0.227*	[0, 0.478]	0.052*
Displacement	0.151	[0, 0.382]	0.146
Straightness	0.127	[0, 0.399]	0.192
Mean Cosine	0.200	[0, 0.444]	0.077
Average Bout Duration	0.211	[0, 0.466]	0.067
Time Spent Moving (%)	0.234*	[0, 0.486]	0.047*
Average Speed	0.362*	[0.013, 0.526]	0.021*

Table 1. Values of the repeatability value, r, for the calculated parameters, along with the 95% confidence intervals (CIs). Values marked with the asterisk (*) indicate significant results ($p < 0.05$)

Figure 1

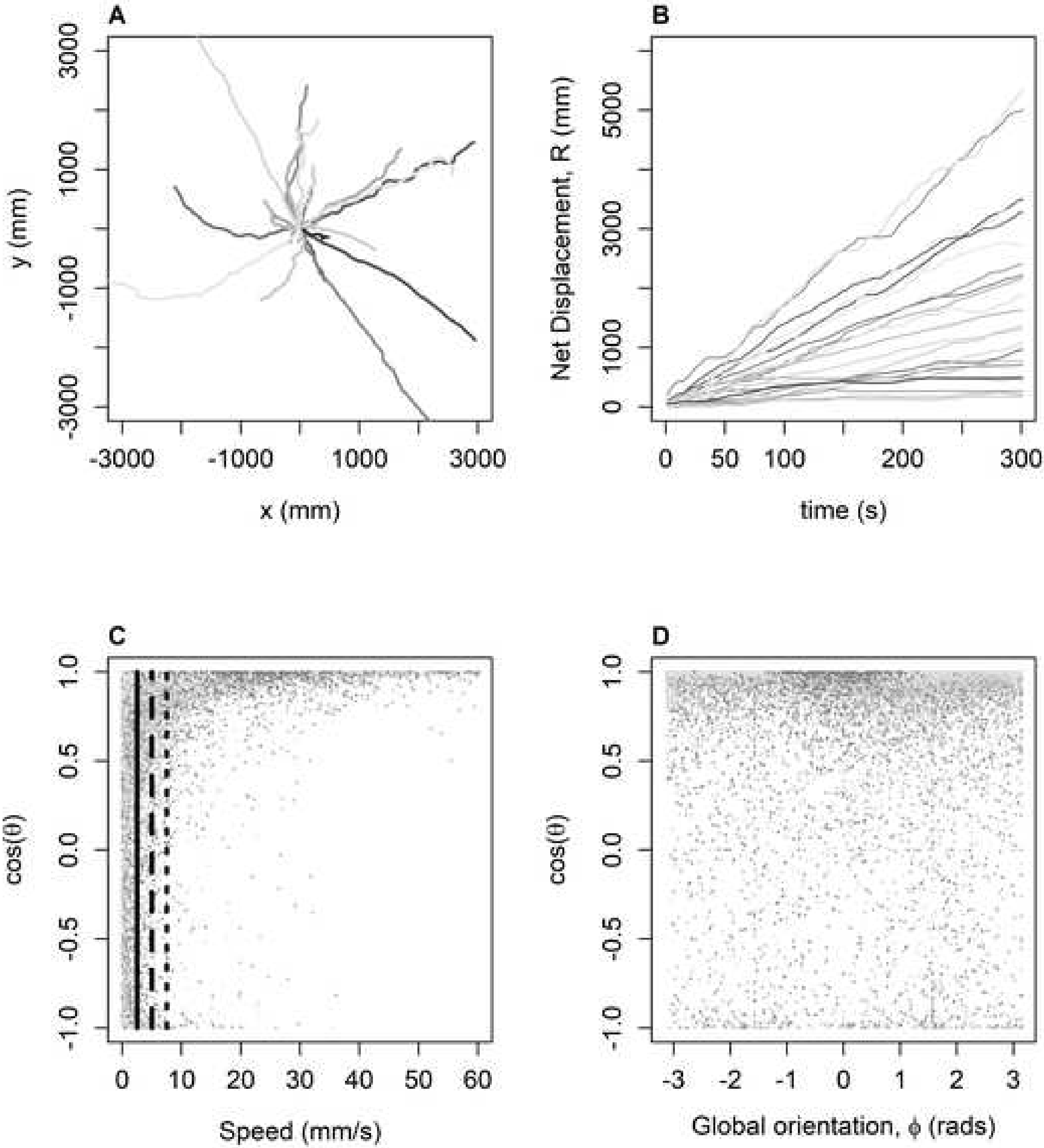
A
y (mm)
3000
1000
-1000
-3000
-3000
-1000
1000
3000
x (mm)
B
Net Displacement, R (mm)
5000
3000
1000
0
0
50
100
200
300
time (s)
C
cos(θ)
1.0
0.5
0.0
-0.5
-1.0
0
10
20
30
40
50
60
Speed (mm/s)
D
cos(θ)
1.0
0.5
0.0
-0.5
-1.0
-3
-2
-1
0
1
2
3
Global orientation, ϕ (rads)

Figure 2

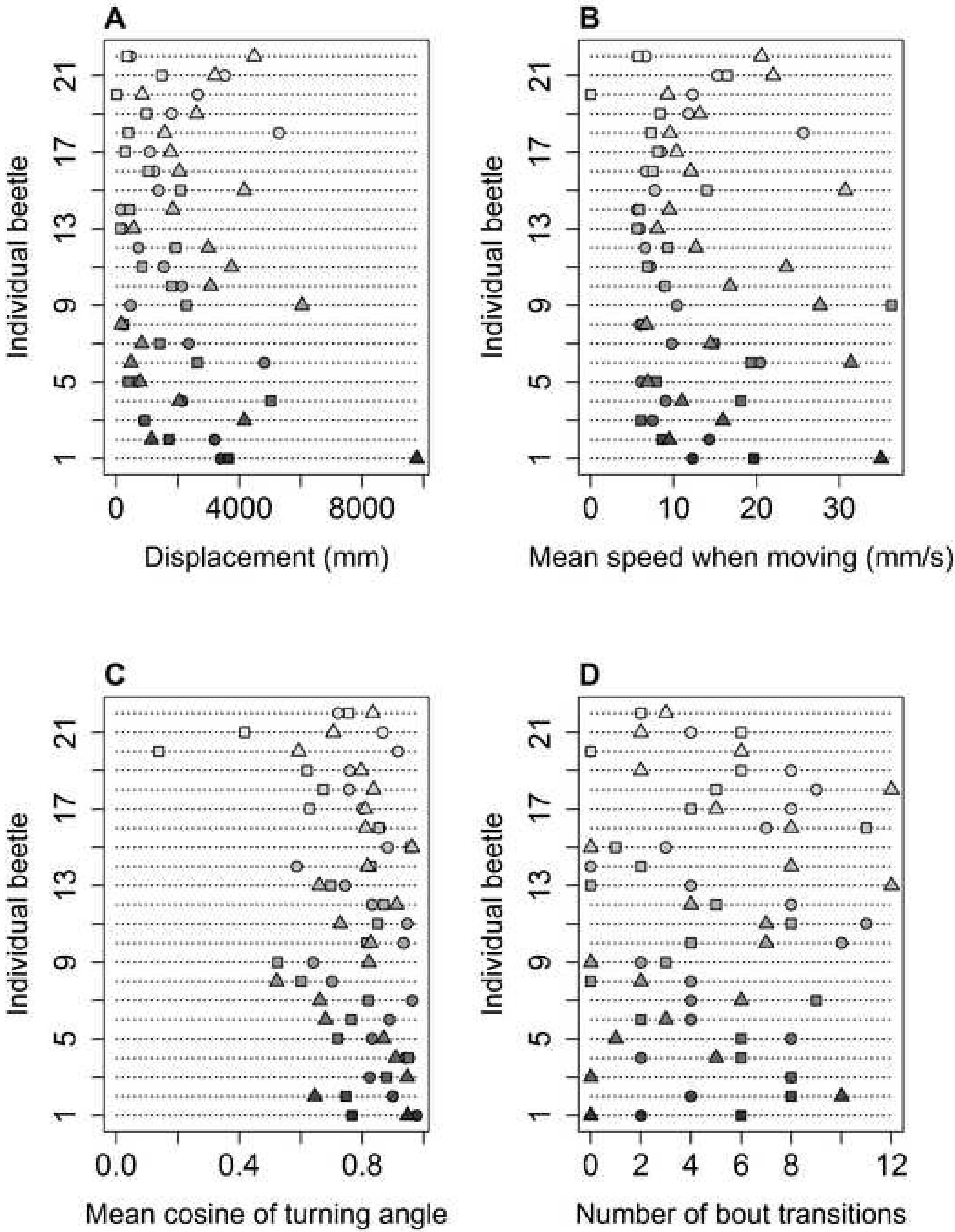
A
B
C
D
Individual beetle
1
5
9
13
17
21
0
4000
8000
Displacement (mm)
0
10
20
30
Mean speed when moving (mm/s)
0.0
0.4
0.8
Mean cosine of turning angle
0
2
4
6
8
12
Number of bout transitions

Figure 3

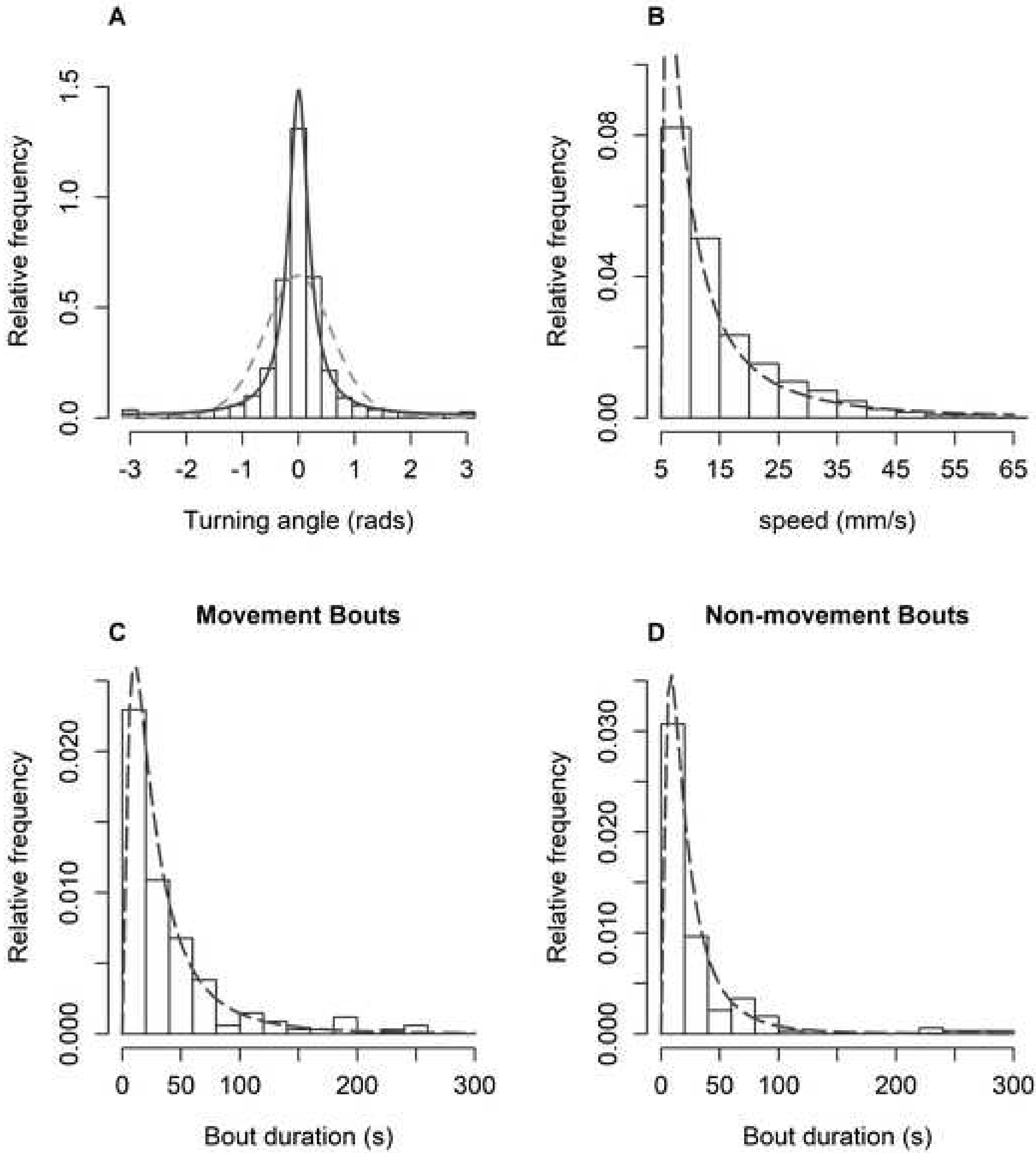
A
Relative frequency
0.0
0.5
1.0
1.5
-3
-2
-1
0
1
2
3
Turning angle (rads)
B
Relative frequency
0.00
0.04
0.08
5
15
25
35
45
55
65
speed (mm/s)
Movement Bouts
C
Relative frequency
0.000
0.010
0.020
0
50
100
200
300
Bout duration (s)
Non-movement Bouts
D
Relative frequency
0.000
0.010
0.020
0.030
0
50
100
200
300
Bout duration (s)

Figure 4

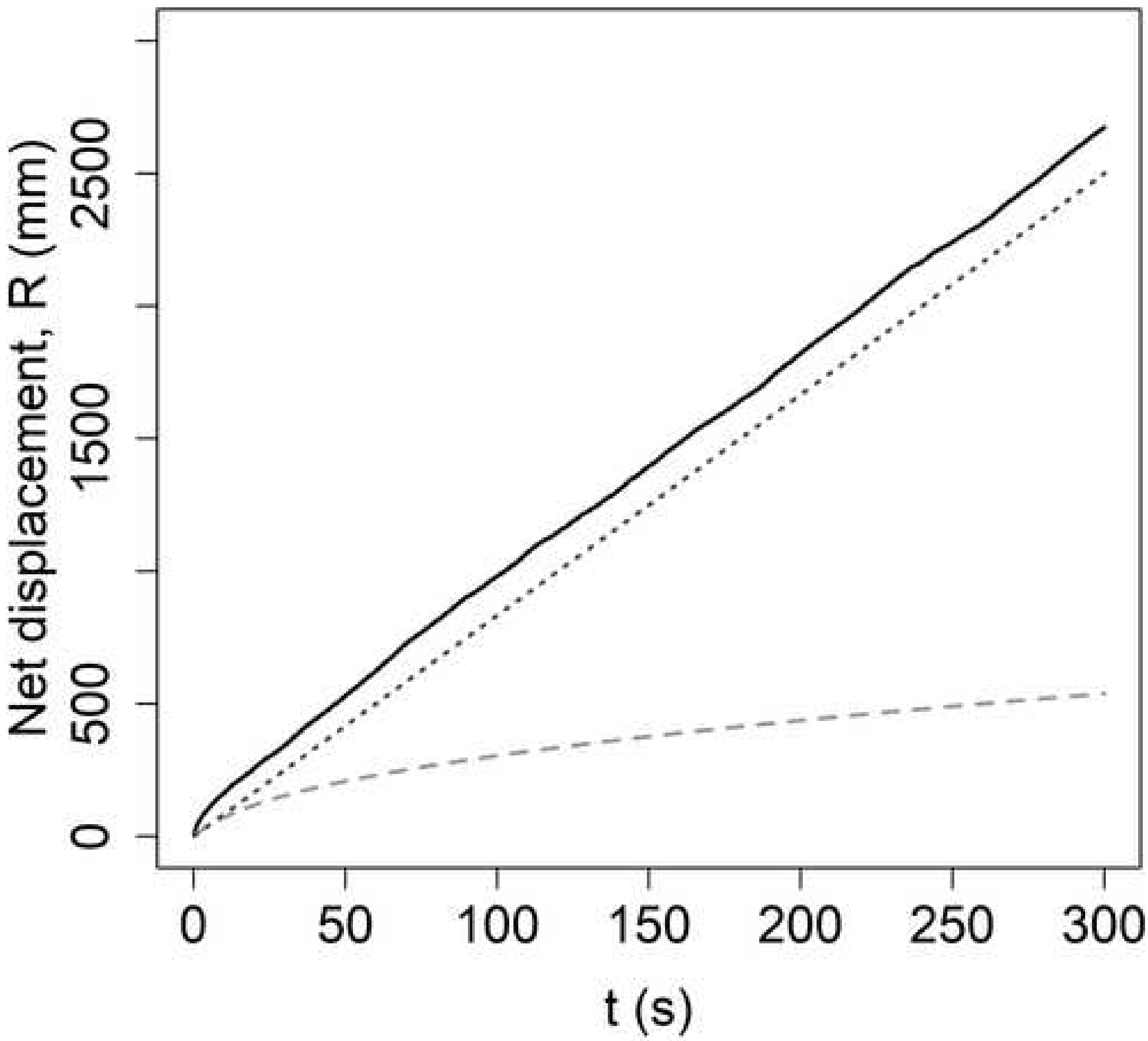
Net displacement, R (mm)
0
500
1500
2500
0
50
100
150
200
250
300
t (s)

Additional file 1

Bout classification

The method to determine the transition between movement and non-movement bouts is an adjusted version of the algorithm described in [1]:

Smoothing Algorithm

1. *Cumulative sum.*

   Determine the cumulative sum

   $C_\tau = \sum_{t=2}^{\tau} S_t$, with $C_1 = S_1$

   for $\tau = 2, \dots, T$.

   Where C_τ denotes the cumulative sum of S_τ at time step τ and is calculated as:

   $$S_t = \begin{cases} S_{t-1} + v_t, & if\ v_t > speed\ threshold\ value \\ S_{t-1} - v_t\ , & if\ v_t \leq speed\ threshold\ value \end{cases}$$

   where v_t is the instantaneous speed calculated at time t.

2. *Time Series*. Construct the time series C_τ vs. τ.
3. *Termination criterion.* Does a turning point exist within the generated time series?

   - Yes: proceed to *4*.

   - No: one cannot effectively analyse this movement path; terminate procedure.

4. *Max-min algorithm.* Determine turning points of the time series using the max-min algorithm (see Appendix 2 in [1]) for full algorithm). Essentially, here the algorithm aims to find turning points (local maxima or minima) in the time series C_τ vs. τ. To do this a moving window of size ε is applied to the time series and for the case when $C_{\tau+\varepsilon} < C_\tau$ a change is determined to have occurred if for the current maximum value of the cumulative sum at time τ, $C_{\tau_{max}}$, we have $\max\{C_{\tau+1}, C_{\tau+2}, \dots, C_{\tau+\varepsilon}\} < C_{\tau_{max}}$ otherwise $C_{\tau_{max}}$ is set at this max value and the method continues starting now at $\tau + 1$ (and similar for $C_{\tau+\varepsilon} > C_\tau$ finding a local minimum). Therefore, in essence the value ε represents the minimum size of a possible bout

and is calculated by the algorithm to give the optimal value for identifying true transition behaviour.

5. *Conclusion*. Classify turning points as either transitions from movement to stationary behaviour or vice-versa.

An example of the results of using this algorithm is demonstrated in Additional File 1, Figure S1.

This algorithm requires calculating a value for the minimum possible length of a bout, ε, per beetle per experimental trial, which was found to range from 3 to 17. As this value was not fixed for all experimental trials, results were also calculated when using a fixed ε across all trials (calculated as the median value of all ε, which in the case for the sampling rate being 1Hz and the speed threshold taking value 5mm/s gave, $\varepsilon = 7$). However, this was not seen to significantly affect the outcome of the analysis (Additional File 1, Table S1-S2).

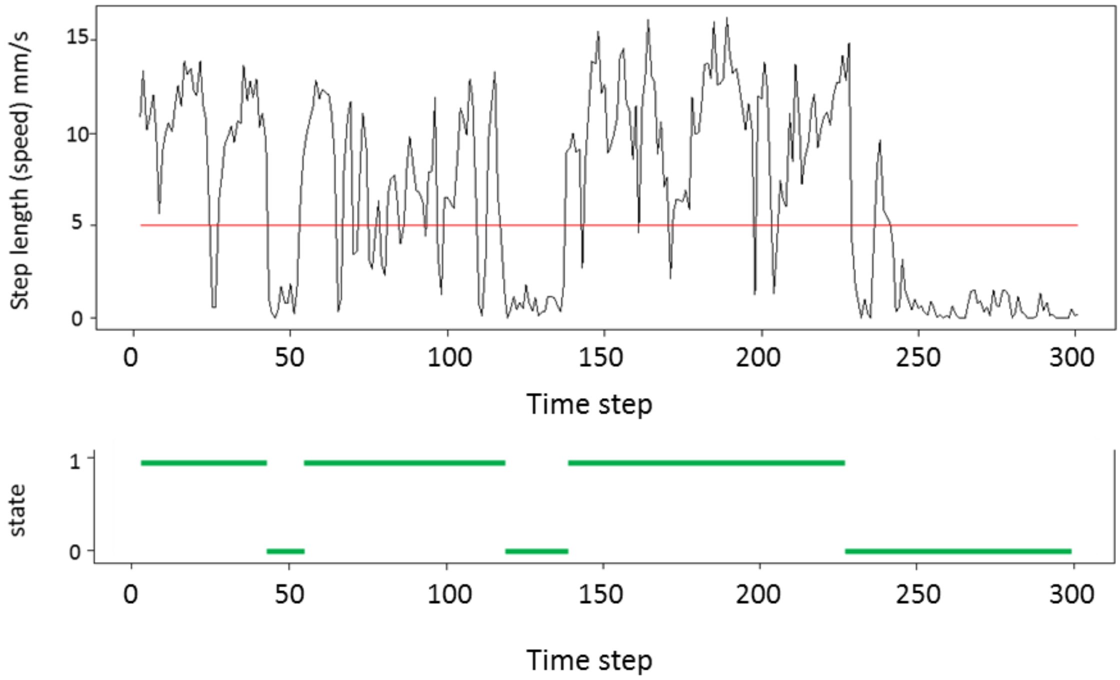

Figure S1 Variation in instantaneous speed over time for a single trial of an example beetle. The red horizontal line represents the speed threshold value of 5 mm/s, which was used throughout the main analysis (other values were considered but did not qualitatively change the results; see Additional File 2). The lower plot demonstrates how the smoothing algorithm designated bouts of movement (state 1) and non-movement (state 0). The sampling rate used was 1 Hz.

	Restricted Power-law		Exponential	Weibull		Log-normal	
Type of bout	x_{min}	A	λ (rate)	γ (shape)	α (scale)	μ (mean)	σ^2 (s.d.)
All	1	1.33	0.028	0.97	35.41	3.07	0.94
Moving	1	1.28	0.016	0.96	47.55	3.39	1.06
Stationary	1	1.31	0.020	0.97	32.97	3.10	0.99

Table S1 Parameter values for the best fit distributions when the median ε value was used in the smoothing algorithm. Results shown are for same sampling rate of 1 Hz and threshold value of 5 mm/s as was used throughout the analysis in the main text

Bout type	Restricted Power law					Exponential					Weibull					Log-normal				
	G^2-Test		K-S Test		AIC	G^2-Test		K-S Test		AIC	G^2-Test		K-S Test		AIC	G^2-Test		K-S Test		AIC
	stat	p	stat	p		stat	p	stat	p		stat	p	stat	p		stat	p	stat	p	
All	119.70	0	0.419	0	3444	33.016	0.005	0.207	0	2991	31.000	0.009	0.177	0	2988	27.314	0.026	0.117	0	2932
Moving	73.15	0	0.366	0	1828	17.358	0.298	0.148	0	1568	18.054	0.260	0.158	0	1571	10.334	0.798	0.092	0.112	1553
Stationary	138.04	0	0.467	0	1599	51.802	0	0.284	0	1419	43.382	0	0.200	0	1409	37.514	0.001	0.142	0.002	1401

Table S2 Results of the statistical tests for each best fitting distribution when the median ε value was used in the smoothing algorithm. Results shown are for the same sampling rate of 1Hz and threshold value of 5 mm/s as was used throughout the analysis in the main text. These results show that the favoured distribution was the log-normal for the distribution of movement bouts, stationary bouts and combined movement and stationary bouts. Comparing these with the findings with a varying epsilon (see Main Text; Additional File 3) shows no qualitative difference.

References

1. Knell AS, Codling EA. Classifying area-restricted search (ARS) using a partial sum approach. Theor Ecol. 2012;5:325–39.

Additional file 2

Summary Statistics Comparison

The summary statistics discussed in section 2.3 (and not included in Figure 3) of the main text are displayed here highlighting the variation across individuals as well as between individuals. The three tables (Additional File 2, Table S1-S3) show the full results of the repeatability analysis, the correlation between individuals and the correlation within individuals.. All tests are for a sampling rate of 1 Hz and speed threshold value of 5 mm/s.

Figure S1 (A-C) variability in the statistical parameters described in the main text section 2.3.2 for each individual trial run per beetle; (A) Time spent moving, (B) Variance in Bout Duration and (C) average length of bouts. (D - E) lengths of bouts of movement and stationary resepctively.

In all plots, circle points correspond to trial 1, squares to trial 2 and triangles to trial 3.

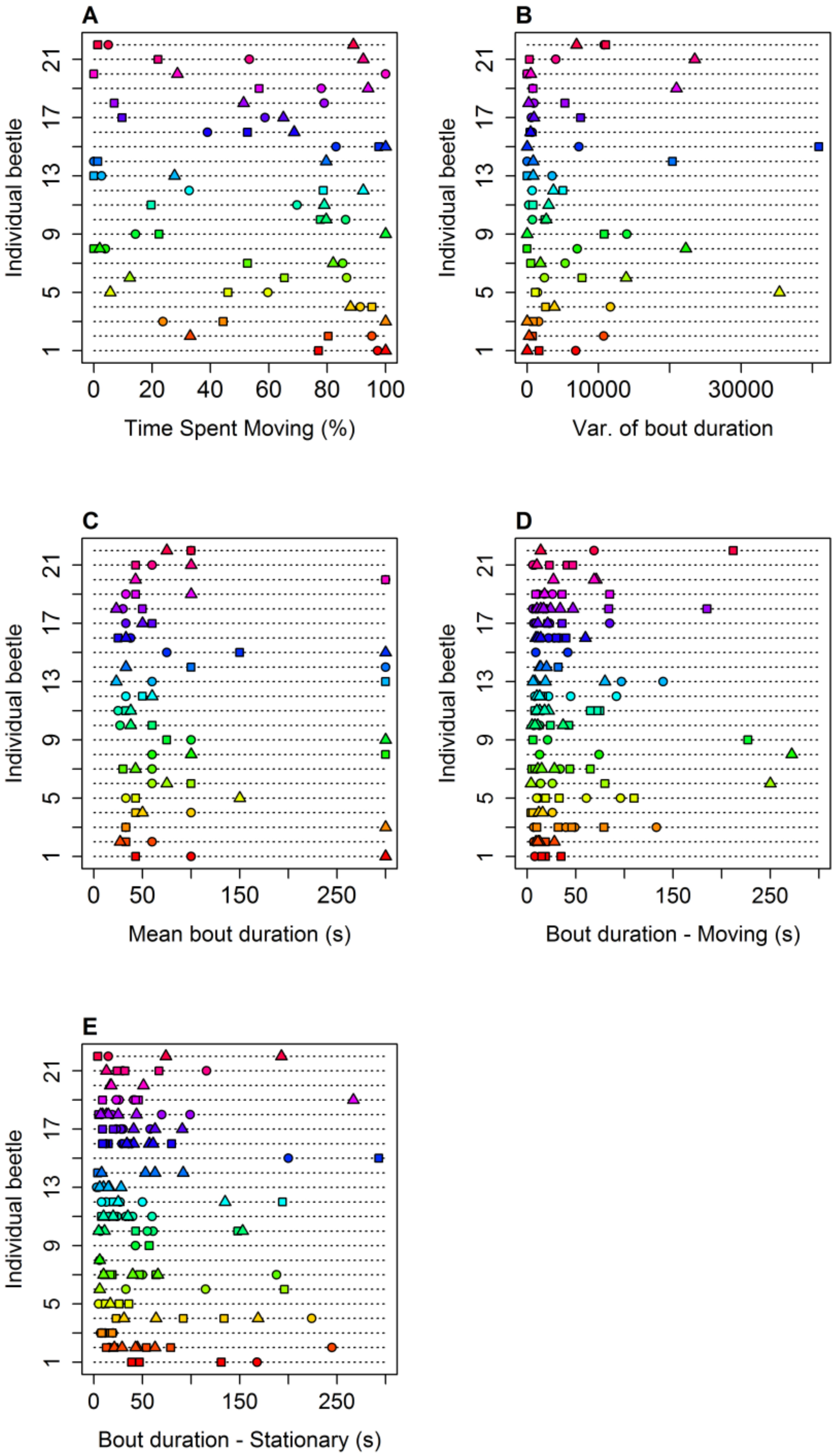

A
Individual beetle
1
5
9
13
17
21
0
20
40
60
80
100
Time Spent Moving (%)
B
Individual beetle
0
10000
30000
Var. of bout duration
C
Individual beetle
0
50
150
250
Mean bout duration (s)
D
Individual beetle
0
50
150
250
Bout duration - Moving (s)
E
Individual beetle
0
50
150
250
Bout duration - Stationary (s)

Figure S1

	Repeatability			V_{ind}	V_{ε}
	r stat	***CI (95%)***	**p-value**		
Number of Bouts	0.227	*[0, 0.478]*	0.052	0.224	0.763
Displacement	0.151	*[0, 0.382]*	0.146	0.164	0.817
Straightness	0.127	*[0, 0.399]*	0.192	0.130	0.870
Mean Cosine	0.200	*[0, 0.444]*	0.077	0.204	0.797
Av. Bout Duration	0.211	*[0, 0.466]*	0.0665	0.208	0.805
Time Spent Moving (%)	0.234*	*[0, 0.486]*	0.0467*	0.237	0.768
Av. Speed	0.362*	*[0.013, 0.526]*	0.0206*	0.331	0.583

Table S1 Values of the repeatability given as $r = V_{\text{ind}}/(V_{\text{ind}} + V_{\varepsilon})$ for the calculated parameters, along with the 95% CIs. Values marked with an asterisk (*) indicate significant results ($p < 0.05$), however, only the Av. Speed Cis did not include 0 therefore, the significant of the results is inconclusive. V_{ind} gives the variance between individuals and V_{ε} the residual (error) variance, equivalent to the variation within individuals.

Correlations	Number of Bouts	Displacement	Straightness	Mean Cosine	Av. Bout Duration T	Time Spent Moving (%)	Av. Speed
Number of Bouts	\\\\\	-0.006	0.301	0.332	-0.129	0.141	-0.291
Displacement	(-0.848, 0.812)	\\\\\	0.229	0.102	0.08	0.287	0.487
Straightness	(-0.555, 0.991)	(-0.673, 0.977)	\\\\\	0.095	-0.089	0.164	0.171
Mean Cosine	(-0.446, 0.987)	(-0.780, 0.837)	(-0.791, 0.848)	\\\\\	-0.072	0.206	-0.03
Av. Bout Duration T	(-0.851, 0.755)	(-0.723, 0.908)	(-0.876, 0.761)	(-0.857, 0.767)	\\\\\	0.101	-0.139
Time Spent Moving (%)	(-0.676, 0.900)	(-0.646, 0.967)	(-0.729, 0.924)	(-0.697, 0.958)	(-0.698, 0.892)	\\\\\	0.258
Av. Speed	(-0.940, 0.449)	(-0.450, 0.993)	(-0.659, 0.910)	(-0.879, 0.711)	(-0.893, 0.587)	(-0.534, 0.943)	\\\\\

Table S2 Correlations between parameters calculated at between individual level using the mixed effects model described in section 2.3.3 in the Main Text. Values in the upper triangle are the correlation coefficients and lower triangle values are the corresponding 95% CIs. Values marked with an asterisk (*) denote those which are significant as the CIs do not straddle 0.

Correlations	Number of Bouts	Displacement	Straightness	Mean Cosine	Av. Bout Duration T	Time Spent Moving (%)	Av. Speed
Number of Bouts	\\\\\	-0.195	0.195	-0.031	-0.657*	0.004	-0.116
Displacement	(-0.445, 0.074)	\\\\\	0.564*	0.535*	0.189	0.747*	0.722*
Straightness	(-0.065, 0.463)	(0.384, 0.745)*	\\\\\	0.644*	-0.24	0.579*	0.241
Mean Cosine	(-0.318, 0.258)	(0.340, 0.743)*	(0.468, 0.801)*	\\\\\	-0.006	0.666*	0.228
Av. Bout Duration T	(-0.819, -0.496)*	(-0.093, 0.461)	(-0.487, 0.033)	(-0.290, 0.271)	\\\\\	0.011	0.176
Time Spent Moving (%)	(-0.272, 0.289)	(0.614, 0.860)*	(0.388, 0.753)*	(0.508, 0.823)*	(-0.274, 0.290)	\\\\\	0.425*
Av. Speed	(-0.418, 0.170)	(0.582, 0.856)*	(-0.022, 0.508)	(-0.061, 0.501)	(-0.102, 0.466)	(0.186, 0.670)*	\\\\\

Table S3 Correlations between parameters calculated at the within individual level using the mixed effects model described in section 2.3.3 in the Main Text. Values in the upper triangle are the correlation coefficients and lower triangle values are the corresponding 95% CIs. Values marked with an asterisk (*) denote those which are significant as the CIs do not straddle 0.

Additional file 3

Complete data analysis for all sampling rates and speed thresholds

Results detailed here include fitting distributions to the turning angles (Additional File 3, Tables S1-S2), instantaneous speeds (Additional File 3, Tables S3-8) and bout durations (Additional File 3, Tables S9-S10) for all combinations of the sampling rates (2 Hz, 1 Hz, 0.5 Hz and 0.2 Hz) and speed threshold (15 mm/s, 10 mm/s 5 mm/s and no threshold value). In the case of the turning angles (Additional File 3, Tables S1-S2), neither the Kuiper nor the Watson tests accepted either the wrapped Cauchy or the wrapped normal distributions. However, when comparing between the two, the AIC preferred the wrapped Cauchy distribution in all cases, and visual comparison confirmed that the wrapped Cauchy was a closer fit to the data.

Comparing the instantaneous speeds at differing sampling rates and speed thresholds, the results reveal that there was no clear likely best-fit distribution, as the preference for a particular distribution varied based on the speed threshold value regardless of the sampling rate; with a propensity for exponential and Weibull distributions when the speed threshold is high and a log-normal distribution for lower values of the threshold. Additional File 3, Tables S3-S5. present the results of fitting distributions to the tail of the data, that is the data which was greater than the optimal x_{min} value of the best-fit power law distribution, which was used to infer the presence of a heavy-tailed distribution. As was mentioned in the main text (Section 3.2), the findings indicate that at any sampling rate and threshold value the power-law was not favoured over the other distributions.

In comparing the bout durations, distributions were considered for the length of moving bouts only, stationary bouts only and both moving and stationary combined. Additional File 3, Tables S9-S10 Indicate that both the log-normal or Weibull distributions were accepted for certain combinations of the sampling rate and speed threshold, although, the AIC generally favoured the log-normal distribution over the Weibull. Data was not considered for no threshold value as this resulted in no stationary bouts (section 2.3.1 of the main text). Similarly, when the threshold value was too high (15 mm/s) or the sampling rate too low (0.2 Hz) the number of bouts measured was too small to give meaningful or accurate results and so have been omitted. Although, discerning an appropriate distribution for the frequency of the bouts was not clear, an inverse relationship between the lengths of consecutive bouts was observed (Additional File 3, Figure S1A). That is, longer bouts were followed by shorter ones and vice versa, and medium length bouts were followed by bouts of similar length. Although (Additional File 3, Figure S1B-C), demonstrates that this is an expected result given the distribution found which best describes the bout lengths.

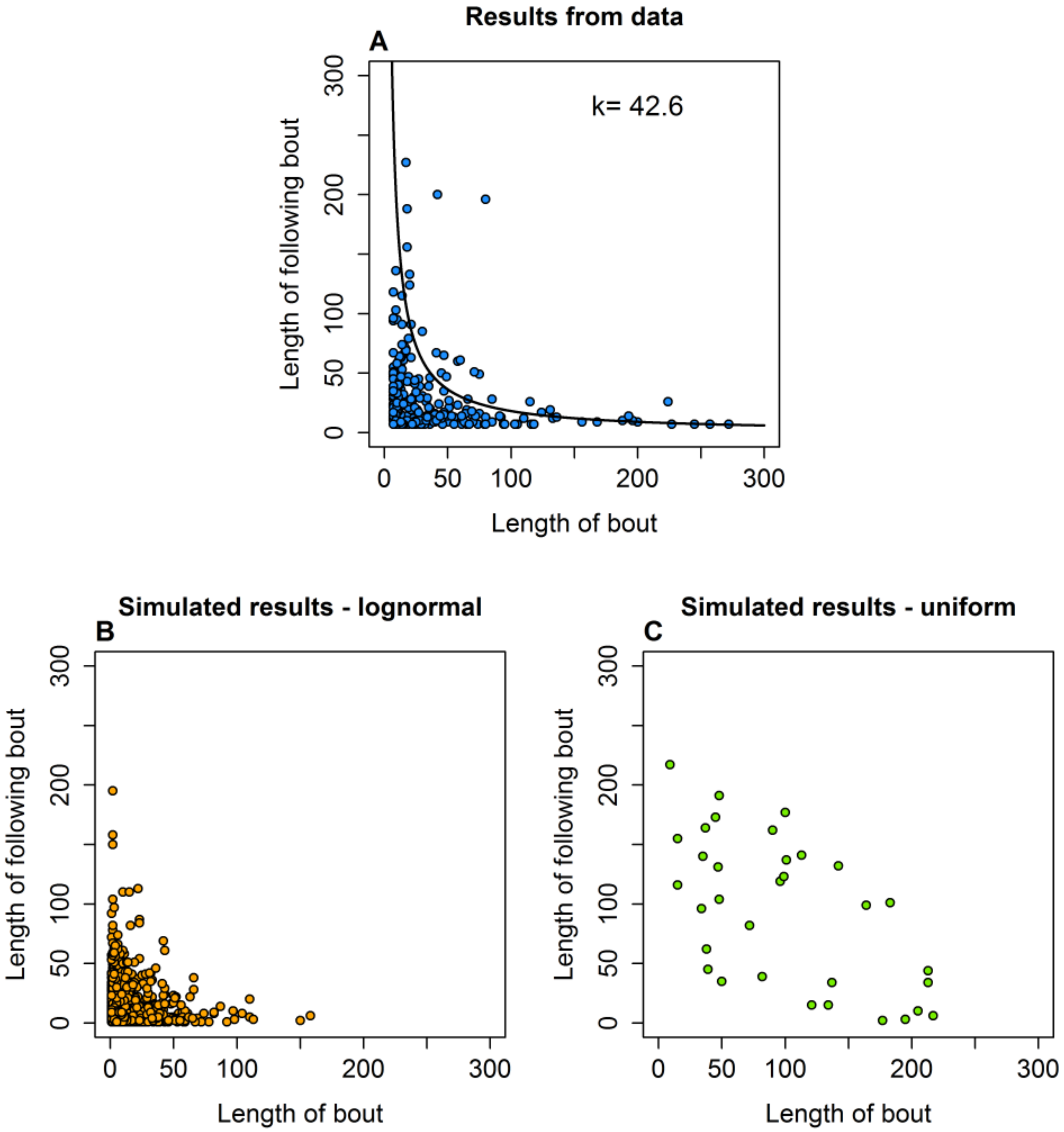

Figure S1 Comparing the lengths of following bouts. **(A)** displays the length of a completed bout compared to the length of the following completed bout, taken from the beetle data. The curve plotted in black shows the line of form k^2/x, where k is a constant shown in top right hand corner of the plot, which accounts for 90% of the plot points being located between the curve and the axes. Comparing this inverse relationship with the expected results from simulated models where the lengths of bouts were drawn from the best fitting log-normal distribution **(B)** and a uniform distribution **(C)** shows the similarity between the actual results and predicted log-normal results. This demonstrates that this inverse relationship between bout lengths is most likely due to the lognormal distribution of the lengths of bouts. Data was calculated with a sampling size of 1 Hz and speed threshold of 5 mm/s,

			Wrapped Cauchy					von Mises				
			Watson test		Kuiper test			Watson test		Kuiper test		
Sampling rate (Hz)	**Speed cut-off (mm/s)**	**Number of points**	**statistic (U^2)**	**p-value**	**statistic (V)**	**p-value**	**AIC**	**statistic (U^2)**	**p-value**	**statistic (V)**	**p-value**	**AIC**
2	none	39534	37.045	<0.01	29.148	<0.01	71744.16	342.2524	<0.01	54.7352	<0.01	95325.86
	5	20155	2.8369	<0.01	7.0981	<0.01	20356.18	125.6914	<0.01	32.6401	<0.01	29315.92
	10	12223	3.2087	<0.01	7.4731	<0.01	7318.787	71.0998	<0.01	24.7016	<0.01	12412.84
	15	7028	2.1223	<0.01	6.0109	<0.01	3007.066	37.4251	<0.01	18.1023	<0.01	5641.406
1	none	19734	8.8988	<0.01	14.7254	<0.01	32661.86	164.3228	<0.01	38.0826	<0.01	44129.71
	5	10011	2.4193	<0.01	6.7936	<0.01	7031.784	51.9381	<0.01	21.0598	<0.01	10668.31
	10	5900	1.9623	<0.01	6.1516	<0.01	2181.849	29.1009	<0.01	15.7044	<0.01	4249.526
	15	3356	1.1261	<0.01	4.7802	<0.01	966.559	16.2974	<0.01	11.9061	<0.01	2129.47
0.5	none	9834	1.9588	<0.01	7.6059	<0.01	16403.39	61.9318	<0.01	23.4196	<0.01	20787.61
	5	5040	1.2417	<0.01	4.7511	<0.01	4275.96	18.824	<0.01	12.9362	<0.01	5454.31
	10	2900	0.9912	<0.01	4.4125	<0.01	1580.272	9.9763	<0.01	9.4965	<0.01	2181.111
	15	1580	0.6161	<0.01	3.5536	<0.01	724.7004	5.1869	<0.01	6.8364	<0.01	1036.83
0.2	none	3894	0.3281	<0.01	2.8823	<0.01	7747.179	14.2082	<0.01	11.559	<0.01	8803.505
	5	2024	0.4467	<0.01	3.068	<0.01	2501.256	5.3992	<0.01	7.018	<0.01	2772.177
	10	1131	0.2489	0.01 < p < 0.025	2.6106	<0.01	1114.658	3.0138	<0.01	5.3566	<0.01	1252.11
	15	604	0.1187	> 0.10	2.0013	<0.01	535.0097	1.5012	<0.01	3.9792	<0.01	584.0033

Table S1. Statistical test results for the turning angle distributions at all considered sampling rates and speed threshold values.

Sampling rate (Hz)	Speed cut-off (mm/s)	Wrapped Cauchy		von Mises	
		μ	**ρ**	**μ**	**κ**
2	none	-0.001	0.814	-0.0108	2.1842
	5	0.0026	0.8413	0.0041	4.5583
	10	0.0049	0.8653	0.0055	6.7311
	15	0.0028	0.8745	0.0037	8.192
1	none	0	0.8192	-0.0108	2.1842
	5	0.0045	0.8586	0.0011	6.4313
	10	0.0053	0.8768	0.0085	8.8482
	15	0.0026	0.8814	0.0024	9.5947
0.5	none	-0.0001	0.8049	0.0019	2.7213
	5	0.0066	0.8466	0.0094	6.3378
	10	0.0105	0.8649	0.0135	8.5942
	15	-0.0034	0.8694	0.0031	9.4126
0.2	none	0.0061	0.7553	0.0175	2.4435
	5	0.0004	0.8154	0.0189	4.9129
	10	0.0042	0.8365	0.0207	6.2121
	15	-0.0085	0.8454	0.0006	7.0781

Table S2 MLE for the parameters of the Wrapped Cauchy and von Mises distributions when considering the turning angle distribution for all considered sampling rates and speed threshold values.

			Power-law (MLE)				Exponential			Weibull			Log-normal		
Sampling rate (Hz)	**Speed cut-off (mm/s)**	**Number of points**	**x_{min}**	**K-S Statistic**	**p-value**	**AIC**	**K-S Statistic**	**p-value**	**AIC**	**K-S Statistic**	**p-value**	**AIC**	**K-S Statistic**	**p-value**	**AIC**
2	none	1473	34.4	0.0517	0	9565	0.0326	0.087	9481	0.0334	0.075	9481	0.0762	0	9835
	5	1506	33.2	0.056	0	9788	0.0321	0.09	9690	0.0327	0.08	9691	0.0767	0	10059
	10	1422	33.8	0.0691	0	9250	0.0344	0.07	9139	0.0348	0.064	9141	0.0783	0	9467
	15	1537	33	0.0718	0	10073	0.0306	0.112	9909	0.0318	0.089	9909	0.0724	0	10297
1	none	6047	10.7	0.0715	0	40149	0.0406	0	39710	0.0275	0	39698	0.0594	0	40699
	5	5499	10.7	0.1027	0	37477	0.0416	0	36196	0.0245	0.003	36178	0.0694	0	37319
	10	620	33.7	0.0576	0.032	3827	0.0332	0.503	3784	0.0344	0.454	3785	0.0713	0.004	3898
	15	608	33.9	0.0647	0.012	3758	0.0343	0.473	3707	0.0351	0.443	3708	0.0731	0.003	3829
0.5	none	2884	10.1	0.0698	0	19110	0.0464	0	18630	0.0339	0.003	18626	0.0601	0	19161
	5	2711	10.6	0.099	0	18176	0.0472	0	17546	0.0359	0.002	17543	0.0633	0	18039
	10	265	33.7	0.0547	0.402	1550	0.0445	0.672	1532	0.0444	0.674	1534	0.0834	0.05	1588
	15	286	33.1	0.0608	0.237	1688	0.0394	0.766	1663	0.0399	0.752	1665	0.0773	0.066	1739
0.2	none	1201	10.6	0.0744	0	7591	0.039	0.052	7558	0.0346	0.114	7560	0.0633	0	7761
	5	596	15.3	0.1058	0	3940	0.0525	0.075	3813	0.0438	0.202	3811	0.0833	0.001	4009
	10	232	24.9	0.1269	0.001	1445	0.0868	0.061	1401	0.0635	0.307	1394	0.1132	0.005	1458
	15	225	25.2	0.1414	0	1408	0.0885	0.059	1353	0.066	0.282	1347	0.1182	0.004	1412

Table S3 Statistical test results for the instantaneous speed distribution at every considered sampling rate and speed threshold value, for the tail of the data only (calculated from the x_{min} value given by the power-law distribution).

Sampling rate (Hz)	Speed cut-off (mm/s)	Number of points	Power-law (MLE)		Exponential		Weibull		Log-normal	
			G^2-Stat	p-value	G^2-Stat	p-value	G^2-Stat	p-value	G^2-Stat	p-value
2	none	1473	97.566	0	54.64	0	53.615	0	190.7	0
	5	1506	112.64	0	58.968	0	58.061	0	201.06	0
	10	1422	117.29	0	53.266	0	52.863	0	181.8	0
	15	1537	152.07	0	60.955	0	59.907	0	199.73	0
1	none	6047	474.71	0	127.95	0	105.87	0	467.07	0
	5	5499	788.32	0	139.6	0	115.05	0	505.81	0
	10	620	43.795	0	35.258	0.013	36.2	0.009973	71.707	0
	15	608	51.591	0	40.38	0.002916	40.75	0.002605	76.507	0
0.5	none	2884	217.46	0	80.254	0	68.17	0	216.77	0
	5	2711	348.12	0	69.982	0	59.646	0	205.26	0
	10	265	12.721	0.5486	18.402	0.4958	18.35	0.4992	30.416	0.04674
	15	286	14.722	0.3974	13.115	0.8326	13.27	0.8244	27.999	0.08345
0.2	none	1201	73.223	0	38.13	0.005713	35.757	0.0113	66.537	0
	5	596	79.829	0	26.142	0.1263	26.044	0.129	70.962	0
	10	232	37.324	0	24.979	0.1612	22.017	0.2834	39.791	0.003486
	15	225	40.923	0	23.062	0.2346	19.279	0.4391	37.747	0.006391

Table S4 Similar to Additional File 3, Table S3, results of the G-Test for the distribution of instantaneous speed. Results are for the tail of the data only.

Sampling rate (Hz)	Speed cut-off (mm/s)	Number of points	Power-law (MLE)		Exponential	Weibull		Log-normal	
			α	x_{min}	λ (rate)	γ (shape)	α (scale)	μ (mean)	σ^2 (s.d.)
2	None	1473	5.56	34.39	0.109	1.02	9.27	1.65	1.31
	5	1506	4.86	33.2	0.109	1.02	9.24	1.64	1.32
	10	1422	4.37	33.76	0.109	1.02	9.21	1.64	1.31
	15	1537	3.68	32.95	0.108	1.03	9.35	1.66	1.3
1	None	6047	2.69	10.73	0.102	0.96	9.65	1.66	1.33
	5	5499	2.19	10.68	0.101	0.95	9.68	1.65	1.38
	10	620	4.84	33.68	0.129	1.03	7.85	1.49	1.26
	15	608	4.21	33.86	0.129	1.02	7.8	1.48	1.29
0.5	None	2884	2.79	10.11	0.108	0.96	9.15	1.61	1.34
	5	2711	2.22	10.63	0.107	0.97	9.23	1.62	1.34
	10	265	5.42	33.73	0.151	1	6.6	1.29	1.32
	15	286	4.49	33.11	0.149	1.01	6.74	1.32	1.34
0.2	None	1201	2.82	10.55	0.117	0.99	8.5	1.55	1.3
	5	596	2.81	15.33	0.111	1.06	9.2	1.65	1.34
	10	232	3.67	24.91	0.133	1.19	7.94	1.56	1.16
	15	225	3.04	25.24	0.135	1.17	7.8	1.53	1.19

Table S5 Parameter values calculated for the instantaneous speed distribution for the tail of the data only.

			Power-law (restricted) (x_{min}=speed cut-off)			Exponential			Weibull			Log-normal		
Sampling rate (Hz)	**Speed cut-off (mm/s)**	**Number of points**	**K-S Statistic**	**p-value**	**AIC**	**K-S Statistic**	**p-value**	**AIC**	**K-S Statistic**	**p-value**	**AIC**	**K-S Statistic**	**p-value**	**AIC**
2	none	39600	0.1795	0	255834	0.1471	0	229424	0.1359	0	228179	0.2205	0	225598
	5	20188	0.249	0	136383	0.0274	0	125141	0.0253	0	124411	0.0691	0	122780
	10	12244	0.1349	0	81086	0.0417	0	75167	0.0209	0	74862	0.0579	0	74333
	15	7039	0.107	0	49828	0.0245	0	44916	0.0217	0.003	44465	0.078	0	44466
1	none	19800	0.1811	0	128277	0.1202	0	116833	0.1158	0	116233	0.2046	0	114963
	5	10045	0.2418	0	66472	0.0266	0	61302	0.0253	0	60915	0.0692	0	60228
	10	5919	0.2188	0	38818	0.0405	0	35861	0.0281	0	35646	0.0605	0	35445
	15	3365	0.1137	0	23603	0.0328	0.001	21154	0.0276	0.012	20844	0.0857	0	20891
0.5	none	9900	0.1865	0	64725	0.0998	0	59457	0.0938	0	59113	0.195	0	58505
	5	5074	0.2341	0	32856	0.0283	0.001	30309	0.0281	0.001	30078	0.0652	0	29705
	10	2918	0.2122	0	18727	0.046	0	17380	0.0343	0.002	17265	0.0586	0	17158
	15	1591	0.2552	0	11093	0.0492	0.001	9944	0.0316	0.083	9770	0.0979	0	9816
0.2	none	3960	0.1928	0	26104	0.0759	0	24162	0.0806	0	23990	0.1737	0	23783
	5	2058	0.2453	0	13063	0.0254	0.141	12053	0.0288	0.065	11933	0.0699	0	11765
	10	1149	0.2035	0	7087	0.0426	0.031	6630	0.0327	0.17	6581	0.07	0	6543
	15	613	0.2444	0	4057	0.051	0.083	3675	0.0396	0.291	3610	0.0804	0.001	3618

Table S6 Statistical test results for the speed distribution at every sampling rate and speed threshold value, for the whole data set (the x_{min} value was fixed at the speed cut off threshold value)

Speed cut-off (mm/s)	Number of points	Power-law (restricted) (x_{min}=speed cut-off)		Exponential		Weibull		Log-normal	
		G^2-Stat	p-value	G^2-Stat	p-value	G^2-Stat	p-value	G^2-Stat	p-value
none	39600	14849	0	327.23	0	296	0	1232.1	0
5	20188	6158.5	0	191.51	0	172.68	0	1258.7	0
10	12244	4145.9	0	213.83	0	160.31	0	1005.9	0
15	7039	250.82	0	111.24	0	97.322	0	803.59	0
none	19800	7586.6	0	208.37	0	271.91	0	570.9	0
5	10045	3545.2	0	122.2	0	117.36	0	594.79	0
10	5919	2148.3	0	129.82	0	106.78	0	437.15	0
15	3365	103.15	0	73.686	0	48.433	0	372.1	0
none	9900	3818	0	69.769	0	147.03	0	250.02	0
5	5074	1813.6	0	66.227	0	65.857	0	252.52	0
10	2918	981.76	0	75.85	0	64.231	0	212.87	0
15	1591	898.04	0	46.329	0	30.643	0.006218	180.75	0
none	3960	1587.8	0	36.44	0	81.035	0	125.79	0
5	2058	749.94	0	39.072	0	40.523	0	98.501	0
10	1149	384.16	0	28.243	0.01321	22.594	0.06721	60.804	0
15	613	315.25	0	24.079	0.04483	25.19	0.03274	56.18	0

Table S7 Similar to Additional File 3, Table S6, with additional results of the G-Test. Results are for the whole data set.

Sampling rate (Hz)	Speed cut-off (mm/s)	Number of points	Power-law (restricted)		Exponential	Weibull		Log-normal	
			α	x_{min}	λ (rate)	γ (shape)	α (scale)	μ (mean)	σ^2 (s.d.)
2	None	39600	1.502	0	0.118	0.526	5.817	0.445	3.256
	5	20188	1.497	5	0.098	0.988	10.12	1.736	1.277
	10	12244	1.499	10	0.098	0.943	9.979	1.686	1.350
	15	7039	1.470	15	0.089	1.029	11.31	1.851	1.291
1	None	19800	1.509	0	0.121	0.579	6.10	0.620	2.99
	5	10045	1.508	5	0.103	0.992	9.668	1.690	1.28
	10	5919	1.503	10	0.102	0.965	9.687	1.667	1.329
	15	3365	1.475	15	0.094	1.066	10.87	1.826	1.268
0.5	None	9900	1.516	0	0.123	0.638	6.424	0.794	2.732
	5	5074	1.512	5	0.109	0.999	9.200	1.644	1.270
	10	2918	1.517	10	0.108	0.966	9.158	1.609	1.340
	15	1591	1.484	15	0.098	1.100	10.516	1.804	1.267
0.2	None	3960	1.524	0	0.126	0.714	6.731	0.973	2.418
	5	2058	1.530	5	0.116	1.022	8.665	1.597	1.251
	10	1149	1.538	10	0.118	0.973	8.406	1.529	1.320
	15	613	1.509	15	0.110	1.091	9.369	1.689	1.233

Table S8 Parameter values calculated for the speed distribution for the whole data set.

All Bouts			Power-law (restricted)					Exponential					Weibull					Log-normal				
			G^2-Test		K-S Test			G^2-Test		K-S Test			G^2-Test		K-S Test			G^2-Test		K-S Test		
Sampling rate (Hz)	Speed cut-off (mm/s)	x_{min}	Stat	p	stat	p	AIC	stat	p	stat	p	AIC	stat	p	stat	p	AIC	stat	p	stat	p	AIC
2	5	0.5	147.17	0	0.393	0	5593	42.001	0.002	0.163	0	4997	30.068	0.051	0.12	0	4986	33.128	0.006	0.095	0	4852
	10	0.5	79.225	0	0.435	0	5515	38.11	0.006	0.159	0	4892	26.862	0.108	0.154	0	4883	13.855	0.792	0.099	0	4701
1	5	1	117.38	0	0.390	0	3364	29.517	0.058	0.107	0.002	2976	26.562	0.115	0.11	0.001	2977	21.854	0.292	0.072	0.078	2902
	10	1	92.14	0	0.438	0	3542	37.948	0.006	0.163	0	3111	38.141	0.006	0.162	0	3113	32.479	0.028	0.114	0	2986
0.5	5	2	96.196	0	0.398	0	1865	23.963	0.198	0.143	0.001	1612	25.352	0.149	0.108	0.025	1609	20.298	0.377	0.078	0.195	1566
	10	2	78.96	0	0.377	0	1696	31.515	0.035	0.14	0.002	1477	31.099	0.039	0.112	0.022	1474	20.441	0.369	0.06	0.536	1436

Moving Bouts			Power-law (restricted)					Exponential					Weibull					Log-normal				
			G^2-Test		K-S Test			G^2-Test		K-S Test			G^2-Test		K-S Test			G^2-Test		K-S Test		
Sampling rate (Hz)	Speed cut-off (mm/s)	x_{min}	Stat	p	stat	p	AIC	stat	p	stat	p	AIC	stat	p	stat	p	AIC	stat	p	stat	p	AIC
2	5	0.5	141.56	0	0.385	0	2928	37.486	0.007	0.102	0.011	2582	30.537	0.045	0.086	0.05	2582	24.226	0.188	0.08	0.078	2541
	10	0.5	79.666	0	0.432	0	2738	27.555	0.092	0.139	0	2363	32.858	0.025	0.126	0.001	2365	15.397	0.697	0.085	0.054	2292
1	5	1	113.15	0	0.368	0	1760	26.489	0.117	0.083	0.216	1550	24.436	0.18	0.091	0.14	1552	16.895	0.597	0.049	0.837	1525
	10	1	93.094	0	0.453	0	1726	32.261	0.029	0.196	0	1490	41.208	0.002	0.159	0	1488	33.806	0.019	0.094	0.09	1432
0.5	5	2	94.111	0	0.408	0	974	22.783	0.247	0.142	0.041	840	24.251	0.187	0.122	0.117	839	18.24	0.561	0.076	0.642	822
	10	2	80.961	0	0.380	0	804	28.548	0.073	0.156	0.027	695	27.964	0.084	0.102	0.314	693	18.412	0.48	0.068	0.811	673

Non-moving Bouts			Power-law (restricted)					Exponential					Weibull					Log-normal				
			G^2-Test		K-S Test			G^2-Test		K-S Test			G^2-Test		K-S Test			G^2-Test		K-S Test		
Sampling rate (Hz)	Speed cut-off (mm/s)	x_{min}	Stat	p	stat	p	AIC	stat	p	stat	p	AIC	stat	p	stat	p	AIC	stat	p	stat	p	AIC
2	5	0.5	27.703	0.01	0.414	0	2668	100.72	0	0.147	0	2407	60.513	0	0.157	0	2396	44.569	0	0.103	0.011	2300
	10	0.5	55.006	0	0.439	0	2782	107.35	0	0.211	0	2519	58.785	0	0.171	0	2501	43.453	0.001	0.117	0.002	2406
1	5	1	58.884	0	0.417	0	1607	38.405	0.005	0.132	0.009	1420	34.773	0.015	0.141	0.004	1422	29.876	0.053	0.11	0.045	1373
	10	1	83.4	0	0.424	0	1820	73.289	0	0.177	0	1618	64.136	0	0.156	0	1618	55.506	0	0.131	0.004	1553
0.5	5	2	96.775	0	0.408	0	895	29.755	0.055	0.162	0.015	772	31.026	0.04	0.121	0.132	771	19.605	0.419	0.106	0.252	745
	10	2	77.426	0	0.385	0	895	26.728	0.111	0.131	0.09	779	28.235	0.079	0.126	0.11	779	20.212	0.382	0.09	0.457	761

Table S9 Statistical test results for the bout distributions. 4 distributions were considered. Sampling size of 0.2 Hz was not included as there were too few bouts to give reliable results, and similar for speed threshold value of 15 mm/s. The case for no speed threshold was also not considered as the data returned few non-moving bouts. Results are for the data as a whole with the fixed x_{min} value at the minimum non-zero value of the data.

All Bouts

Sampling rate (Hz)	Speed cut-off (mm/s)	Power-law (restricted) α	Power-law (restricted) x_{min}	Exponential λ (rate)	Weibull γ (shape)	Weibull α (scale)	Log-normal μ (mean)	Log-normal $σ^2$ (s.d.)
2	5	0.5	1.30	0.019	0.89	50.23	3.36	1.06
	10	0.5	1.30	0.020	0.91	46.00	3.31	0.97
1	5	1	1.32	0.025	0.96	39.30	3.15	1.00
	10	1	1.34	0.034	1.00	29.77	2.92	0.88
0.5	5	2	1.35	0.038	1.13	27.46	2.87	0.86
	10	2	1.37	0.044	1.13	23.79	2.72	0.87

Moving Bouts

Sampling rate (Hz)	Speed cut-off (mm/s)	Power-law (restricted) α	Power-law (restricted) x_{min}	Exponential λ (rate)	Weibull γ (shape)	Weibull α (scale)	Log-normal μ (mean)	Log-normal $σ^2$ (s.d.)
2	5	0.5	1.28	0.016	0.94	59.52	3.54	1.08
	10	0.5	1.30	0.024	1.04	42.15	3.28	0.89
1	5	1	1.30	0.022	0.97	45.73	3.30	1.04
	10	1	1.35	0.039	1.12	27.07	2.87	0.82
0.5	5	2	1.34	0.035	1.14	30.48	2.97	0.88
	10	2	1.39	0.053	1.20	20.27	2.59	0.81

Non-moving Bouts

Sampling rate (Hz)	Speed cut-off (mm/s)	Power-law (restricted) α	Power-law (restricted) x_{min}	Exponential λ (rate)	Weibull γ (shape)	Weibull α (scale)	Log-normal μ (mean)	Log-normal $σ^2$ (s.d.)
2	5	0.5	1.31	0.022	0.86	41.65	3.19	1.00
	10	0.5	1.30	0.018	0.84	49.76	3.35	1.04
1	5	1	1.33	0.030	0.97	33.13	3.00	0.94
	10	1	1.34	0.030	0.94	32.46	2.98	0.93
0.5	5	2	1.36	0.043	1.14	24.46	2.77	0.81
	10	2	1.35	0.038	1.11	27.39	2.85	0.90

Table S10 MLE for the parameters of the four distributions considered for the distribution of the bout lengths.

Additional file 4

Analysis of data when including truncated bouts

As discussed in the main text (Section 2.3.1), bouts which had not ended by the end of the experiment were not included in the final analysis as their true length was indeterminable. Additional File 4, Tables S1-S2 show the results of the statistical analysis used in the main text when these bouts were included (that is the final bout was deemed to have finished when the experiment had ended) at a sampling rate of 1HZ and speed threshold value of 5mm/s. In general, the inclusion of these truncated bouts resulted in the statistical tests rejecting the fitted distributions, , with the G-test rejecting all distributions for all types of bouts and the K-S test rejecting the distributions for all bout types except for the exponential in the case of stationary bouts, the Weibull in the case of moving bouts and the log-normal for both moving and stationary bouts ($p > 0.1$). However, the log-normal distribution was favoured by the AIC likelihood for all bout types, which is the same for the findings when the truncated bouts were excluded (see Additional File 3; Supplementary Tables S9-S10).

	Restricted Power law					Exponential					Weibull					Log-normal				
	G^2-Test		K-S Test		AIC	G^2-Test		K-S Test		AIC	G^2-Test		K-S Test		AIC	G^2-Test		K-S Test		AIC
Bout type	**stat**	**p**	**stat**	**p**		**stat**	**p**	**stat**	**p**		**stat**	**p**	**stat**	**p**		**stat**	**p**	**stat**	**p**	
All	87.764	0	0.419	0	1726	54.884	0	0.130	0	1574	45.813	0	0.117	0	1537	40.48	0.004	0.065	0.075	1506
Moving	96.500	0	0.568	0	1609	56.667	0	0.104	0.031	1037	50.194	0	0.088	0.174	1017	39.878	0.005	0.042	0.879	993
Non-moving	135.39	0	0.764	0	1809	91.156	0	0.085	0.121	1543	74.918	0	0.093	0.072	1545	54.538	0	0.094	0.164	1500

Table S1 Test results for the bout distributions when truncated bouts were included. 4 distributions were considered. Results are for the data as a whole with the fixed x_{min} value at the minimum non-zero value of the data. Results displayed are for sampling size 1 Hz and speed threshold 5 mm/s, which were the values used throughout the analysis in the main text. The results indicate that the log-normal distribution was the favoured distribution for all types of bouts in similitude with the analysis when the truncated bouts were not included (see Main Text; Additional File 2, Supplementary Tables S9-S10).

Type of bout	Restricted Power-law		Exponential	Weibull		Log-normal	
	x_{min}	α	λ (rate)	γ (shape)	α (scale)	μ (mean)	σ^2 (s.d.)
All	1	1.30	0.019	0.90	48.69	3.32	1.08
Moving	1	1.29	0.018	0.94	54.10	3.44	1.09
Non-moving	1	1.31	0.021	0.87	43.41	3.21	1.07

Table S2 - MLE for the parameters of the four distributions considered for the bout distributions when including truncated bouts. Results are for the data as a whole with the fixed x_{min} value at the minimum non-zero value of the data. Results displayed are for sampling size 1 Hz and speed threshold 5mm/s, which were the values used throughout the analysis in the main text.

Additional File 5

Categorisation of movement paths as a BRW or a CRW

Here we discuss the methods used to categorise the movement of the beetles as either a CRW or a BRW at both the individual and population level.

It was noted in the main text that at the population level a slight preference in global direction was found (section 3.3). However, when looking at the individual level this apparent preferential angle can be explained by comparing the initial orientation of the beetles along with their final positions. Additional File 5, Figure S1A shows the direction of each individual trial run at the beginning of the experiment, represented as a unit vector in the given direction (the direction was calculated by calculating the mean orientation across the first 10 moving steps of the trial). Additional File 5, Figure S1B shows the final location of the beetle for each trial run represented as a unit vector in the direction of the final position. These figures demonstrate that whilst the initial distribution of orientation angles appears to be concentrated towards the top-right quadrant and away from the bottom-left, the final positions of the beetles have become more uniform in distribution. Hence, we conclude that at the population level, there is no consistent long-term global preferred direction of movement, and the slight preference in global orientation found when analysing all steps of the movement paths is due to the initial distribution of movement directions.

A direct method of determining if a movement path is better described by either a CRW or BRW is to calculate the Marsh-Jones Δ-statistic [1] (section 2.3.3); given by:

$$\Delta = \frac{1}{n^2}\left[\left(\sum \cos\theta_i\right)^2 + \left(\sum \sin\theta_i\right)^2\right] - \frac{1}{(n-1)^2}\left[\left(\sum \cos\omega_i\right)^2 + \left(\sum \sin\omega_i\right)^2\right]$$

where, θ_i is the global orientation and ω_i is the turning angle, at time i.

Turning angles are calculated as the angle between the direction of successive steps and the global orientation of a given time step is calculated as the angle between the direction at that time step and the positive y-axis. The expected values of the Δ statistic are calculated by extensive simulations using the equivalent number of data points as found in the observed data, therefore, the value of the statistic depends upon both the number of individuals and the number of time steps. The global orientation and turning angles for these simulations are drawn from distributions with resultant vectors calculated directly from the global orientations and turning angles of the observed data.

The analysis of the results of calculating the Δ-statistic is given in the main text, section 3.3. Additional File 5, Table S1 shows how the Δ statistic classified each individual trial, with 5 trials corresponding to a CRW and only one as a BRW. The remaining trials could not be determined as being either type of random walk.

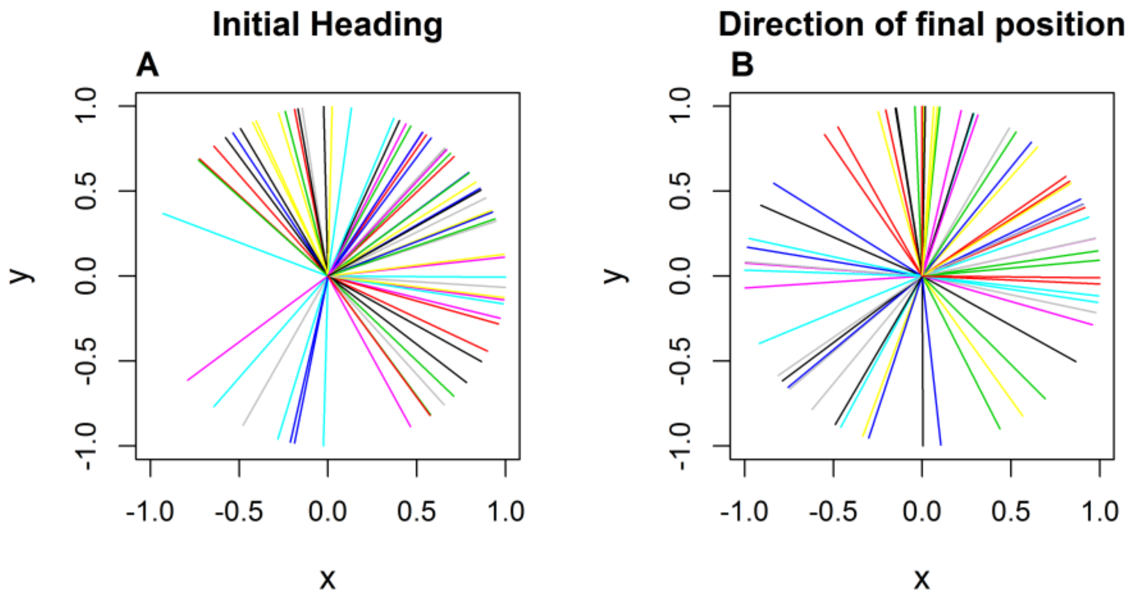

Figure S1 (A) orientation of all the individual trials (shown as a unit vector in the direction of the angle of orientation) at the start of the experiment (orientation was taken as the mean of the first 10 steps of movement). In contrast **(B)** shows the final location of the beetle at the end of the experiment (shown as a unit vector in the direction of the final location). Each individual colour represents an individual beetle, as in Figures in the main text.

Beetle	Trial	∆ observed	Predicted ∆ (BRW)	Predicted ∆ (CRW)
1	1	-0.0151	(-0.0079, 0.0626)	(-1.0111, -0.4215)
2	1	-0.0145	(0.1441, 0.2113)	(-0.7498, -0.6336)
3	1	-0.0779	(0.2214, 0.2385)	(-0.6161, -0.5434)
4	1	-0.1473	(0.1567, 0.2196)	(-0.87, -0.6652)
5	1	0.0433	(0.1669, 0.225)	(-0.644, -0.5636)
6	1	0.0753	(0.1048, 0.1836)	(-0.719, -0.619)
7	1	-0.0954	(0.0751, 0.1594)	(-0.9646, -0.5823)
8	1	-0.2887	(0.0875, 0.1624)	(-0.4506, -0.4046)
9*	1*	-0.4143*	(-0.0077, 0.0266)*	(-0.4263, -0.3827)*
10	1	-0.111	(0.1157, 0.193)	(-0.9065, -0.6538)
11	1	-0.0984	(0.1011, 0.1816)	(-0.9191, -0.6444)
12	1	-0.5412	(0.0486, 0.123)	(-0.6497, -0.5705)
13	1	-0.1998	(0.2153, 0.2386)	(-0.6238, -0.5488)
14*	1*	-0.2871*	(-0.0073, 0.024)*	(-0.2995, -0.2678)*
15	1	-0.3388	(0.205, 0.2378)	(-0.7348, -0.6249)
16	1	0.0768	(0.0845, 0.1659)	(-0.7536, -0.6344)
17	1	-0.3343	(0.1587, 0.2194)	(-0.6182, -0.544)
18	1	-0.0491	(0.2226, 0.2374)	(-0.5038, -0.4521)
19	1	-0.1062	(0.2252, 0.2376)	(-0.5697, -0.5057)
20	1	-0.1286	(0.166, 0.2251)	(-0.8259, -0.664)
21	1	-0.1229	(0.2069, 0.2389)	(-0.7173, -0.6145)
22	1	-0.0939	(0.2208, 0.2378)	(-0.5412, -0.4822)
1	2	-0.1798	(0.1929, 0.2347)	(-0.5347, -0.4768)
2	2	0.0821	(0.2045, 0.2381)	(-0.5134, -0.4588)
3	2	-0.135	(0.2067, 0.2394)	(-0.7297, -0.623)
4†	2†	0.0217†	(0.0147, 0.0929)†	(-0.9175, -0.6462)†
5*	2*	-0.4462*	(-0.0029, 0.0405)*	(-0.4584, -0.4112)*
6	2	0.0636	(0.2094, 0.2395)	(-0.5196, -0.4638)
7	2	-0.1473	(0.2065, 0.2389)	(-0.5373, -0.4801)
8	2	-0.0093	(0.1448, 0.2095)	(-0.2616, -0.2335)
9	2	-0.0559	(0.0417, 0.1143)	(-0.1471, -0.1266)
10	2	0.044	(0.1911, 0.2355)	(-0.5892, -0.5214)
11	2	-0.1272	(0.2225, 0.2392)	(-0.664, -0.5824)
12	2	0.0366	(0.145, 0.2131)	(-0.6917, -0.599)
13	2	-0.2612	(0.0413, 0.1136)	(-0.3539, -0.3173)
14	2	-0.2799	(0.1629, 0.2209)	(-0.5701, -0.5053)
15*	2*	-0.6147*	(0.1713, 0.225)*	(-0.9516, -0.6057)*
16	2	-0.2787	(0.223, 0.2394)	(-0.733, -0.6218)
17	2	0.0369	(0.2183, 0.2394)	(-0.514, -0.4595)
18	2	-0.0736	(0.2257, 0.2379)	(-0.5378, -0.4809)
19	2	-0.0409	(0.1654, 0.2226)	(-0.3359, -0.3026)
20	2	0.1448	(0.155, 0.2182)	(-0.5614, -0.4984)
21	2	-0.06	(0.052, 0.1266)	(-0.1694, -0.1479)
22	2	-0.2325	(0.1278, 0.1987)	(-0.4582, -0.4124)

1	3	0.0031	(0.0236, 0.1048)	(-0.9285, -0.6358)
2	3	-0.19	(0.0999, 0.1751)	(-0.3687, -0.332)
3	3	-0.0977	(0.1002, 0.1805)	(-0.9257, -0.638)
4	3	-0.4701	(0.1812, 0.2301)	(-0.7996, -0.6538)
5	3	-0.0781	(0.1881, 0.2342)	(-0.7211, -0.6184)
6	3	-0.2405	(0.1994, 0.2364)	(-0.8602, -0.6691)
7	3	-0.3289	(0.0534, 0.1279)	(-0.44, -0.3964)
8	3	-0.2201	(0.0247, 0.0903)	(-0.2874, -0.2571)
9	3	-0.1472	(0.2258, 0.2381)	(-0.6678, -0.5791)
10	3	-0.2246	(0.2163, 0.2396)	(-0.6483, -0.5675)
11	3	0.0318	(0.2214, 0.2394)	(-0.4081, -0.3677)
12	3	-0.0704	(0.1298, 0.2031)	(-0.8328, -0.6674)
13	3	-0.1881	(0.149, 0.2128)	(-0.4508, -0.4059)
14	3	-0.0104	(0.2004, 0.2375)	(-0.6207, -0.5484)
15*	3*	-0.7675*	(0.0905, 0.1657)*	(-0.9685, -0.5703)*
16	3	-0.2012	(0.2077, 0.2386)	(-0.5973, -0.5288)
17	3	-0.2774	(0.1496, 0.2133)	(-0.5446, -0.486)
18	3	-0.035	(0.1863, 0.2336)	(-0.6828, -0.5931)
19	3	-0.0879	(0.2185, 0.2394)	(-0.641, -0.5612)
20	3	-0.2363	(0.0296, 0.0989)	(-0.3149, -0.283)
21	3	-0.3461	(0.0783, 0.1555)	(-0.4961, -0.4437)
22	3	-0.1682	(0.2258, 0.2385)	(-0.6897, -0.5979)

Table S1 shows the Δ statistic calculated from the observed movement paths. The intervals for the expected values of the BRW and CRW were calculated via extensive simulation of random walks generated using the same number of steps as observed in the experiment, and represent the 95% significance level for each respective RW type. Therefore, any observed Δ falling outside these intervals can be rejected a the 5% significance level. Those marked with (*) have observed Δ corresponding to a CRW and those with a (†) correspond to a BRW.

References

1. Marsh LM, Jones RE. The form and consequences of random walk movement models. Journal of Theoretical Biology. 1988;133:113–31.